University of Southern Queensland

Faculty of Health, Engineering and Sciences

CFD analysis of Olympic Flat-Water Sprint Kayaking at Variable Conditions.

A dissertation submitted by

Ethan Wyatt

in fulfilment of the requirements of

ENP4111 Professional Engineering Research Project

towards the degree of

Bachelor of Engineering (Honours) (Mechanical)

Submitted: November 2024

This page intentionally left blank.

Abstract

The Purpose of this research is to create a useful CFD model that can calculate performance metrics of a kayak, across a wide range of relevant conditions. First a literature review was conducted, to gain both, a better understanding of relevant theory, as well as to identify the existing research. This allowed for the development of an effective methodology, which would yield results, that where both accurate and useful, filling gaps in the existing knowledge base. The chosen methodology comprised of three major steps, firstly appropriately modelling the relevant geometry, then developing an appropriate multiphase volume of a fluid flatwater simulation, before finally testing at an array of various flow speeds and direction. The resulting data was found to be representative of the expected trends, however showed limited accuracy at flow rates with a magnitude of 15 m/s or higher. Finally, to demonstrate the effectiveness of the model, examples were given outlining its usefulness as both, a race strategy and rapid design analysis tool.

University of Southern Queensland

School of Engineering

ENP4111 Research Project

Limitations of Use

University of Southern Queensland

Faculty of Health, Engineering and Sciences

ENG4111/ENG4112 Research Project

Certification of Dissertation

I certify that the ideas, designs and experimental work, results, analyses, and conclusions set out in this dissertation are entirely my own effort, except where otherwise indicated and acknowledged.

I further certify that the work is original and has not been previously submitted for assessment in any other course or institution, except where specifically stated.

Ethan Wyatt

[redacted]

Acknowledgements

This research has been completed under the principal supervision of Dr Khalid Saleh. I would also like to show appreciation to the UniSQ's eResearch Services and staff, including Richard Young and others, who granted me access to the universities High Performance Computing, research cluster, known as Fawkes. Additionally, my friend Jacob Flemming, for aiding me with the modelling of his own personal kayak.

Contents

List of Tables

List of Figures

1. Introduction

1.1. Background

Throughout human history aquatic travel has played a significant role in the expansion of our species. The earliest recorded civilisations all found success by settling near major rivers, as this gave them access to fresh water, and inevitably resulted in the creation of the canoe, the basis of the modern kayak. As civilisation evolved over time, we found the need to develop larger watercraft, capable of moving cargo. This development has continued to create the large cargo, passenger, and battleship technology we possess currently, however single person watercraft have not changed much at all since there creation, except for material changes.

Kayaks are believed to have first been built approximately 5000 years ago, by tribes in north America. These tribes constructed kayaks out of a variety of materials, such as either bones or wood for the frame, which would have animal skins covering it to make a waterproof hull. Earlier kayaks also generally came in a much greater variance of sizes ranging from shorter hunting kayaks, up to 60-foot kayaks that could carry families, and often used seal bladders for extra buoyancy. (blazinpaddles 2017)

The major development of kayaks has come from competitions, like the Olympic games. At the Berlin Olympic games in 1936, (blazinpaddles 2017) kayak racing was introduced for the first time. At the Olympic games athletes compete in flatwater sprints between 200m and 1000m. (*Canoe Flatwater* 2023) In this style of competition, athletes can be separated by margins far smaller than a second, therefore unlike in the manufacturing of larger vessels, kayaks designed for sports require an extremely high level of accuracy. This is however difficult as a variety of small variables at play, make design extremely challenging, when approaching the limit of performance.

Through the history of the Olympic games between 1972 and 2000 there were 3 major kayak design changes, first the Delta shaped kayak in 1972, then the eagle design in 1988, followed by the modified eagle design in 1996. (Robinson, Holt & Pelham 2002) The introduction of each of these designs, correlates to a major reduction in race times across the 1000 m. This shows just how much kayak design has improved and how great of an effect it has on the level of competition in the sport.

Ambient conditions also have a major impact on race times, and may be affected by the waters current, the wind speed and direction and its effects on the surface of the water. The conditions will determine the hydrodynamic forces acting on the hull and the resulting drag experienced by the kayak. Combining this with biomechanical information relating to the athlete, would allow the CFD model, to be a useful tool in optimising competitive race performance. (Mantha et al. 2013)

1.2. Aims and Objectives

The research being proposed will be to create a Computational Fluid Dynamics (CFD) model, to analyse the effects of dynamic ambient conditions, present during a competitive flatwater kayak sprint, on the overall performance of the kayak. By using the CFD model at an array of conditions, more general analytical models can be generated to determine the relationship between key conditional parameters, such as flow speed, and key performance parameters, such as drag, across the range of expected conditions. This information could be applied to a variety of other applications, race strategies and kayak designs, with some additional information or results.

Race strategy optimisation can be achieved, by combining the results of a CFD model, with biomechanical knowledge of the human body. In the case of kayaker performance, several conditions will affect the success of an athlete during an event, including wind, temperature, water current, elevation, and fatigue. Combining all these external factors into a CFD model, would allow coaches to make informed decisions on strategy, such as recommendations on stroke rate and length, to vary performance across different race lengths. Additionally, assessing the performance of other athletes, could improve energy conservation strategies, for later races throughout an event. By adapting this model to other vessels, such as cargo ships, the model might serve additional use to optimize fuel efficiency in powered watercraft.

Design optimisation can be achieved by generating drag contour maps on the surface of the kayaks hull. Although the kayak has existed a long time, design is mainly iterative, essentially trial and error. Physical testing has limitations, such as consistency during testing, cost of prototype production and generic performance results for the design. By using a drag contour map, designers can get a more localised understanding of exactly where their designs are limited. Assuming an appropriate knowledge of average velocities in kayaking events, design could even be optimised for different length kayaking events. This sort of precision is necessary, as modern design approaches its limits.

1.3. General Methodology

The following is a generic methodology for the research, which is subject to variation. Given many of the following tasks are not fully independent of one another, it is therefore likely that some of them may need to be completed, either out of order or reattempted, depending on the success of others.

1. Create a suitable multiphase CFD model of a body of water, that accurately simulates fluid interactions at the free surface.

2. Create a 3D model of a suitable kayak, using appropriate software tools and measurements from a real kayak.

3. Create a 3D model of a kayaker, making reasonable approximations, regarding both the kayakers shape and size.

4. Combine the various models using suitable modelling methods and tools, to ensure that all the relevant interactions between the models, are appropriately represented in the final model.

5. Use the model to measure the effects of variations in both the magnitude and direction, of ambient conditions, within a reasonable range.

6. Conduct various independence studies, to ensure modelling factors such as mesh and domain sizes are independent of the results.

2. Literature Review

2.1. Overview

Before creating a CFD, model it is important to complete a comprehensive literature review. By considering past literature, it can be determined, what work has already been completed and what the current limitations are, in the specific field. This information can help to focus current research into areas that need further development, due to limitations in the current or past research.

A main area of interest for this project are the effectiveness of current CFD techniques in the nautical space. Understanding how these techniques work, along with where and why they were developed, can help to identify the limits of their usefulness to this project. In the context of a CFD analysis, techniques include modelling, meshing, defining boundary conditions, models, numerical schemes and more.

The other main area of interest for this project, is the contributing factors to kayak performance. Understanding what limits kayak performance is crucial to identifying the limits of models in previous works. A key focus of this project is modelling the effects of ambient race conditions, however there are several key factors to consider when modelling a nautical vessel, such as propulsion forces, drag forces, and geometry to name a few.

Due to the computational requirements often associated with CFD modelling, research ultimately requires a considerable amount of financial support. As a result, most of the nautical based CFD research, is primarily completed in a commercial scope, where the drag of large shipping vessels is a concern because of its effect on the fuel economy of the vessel, or in some sporting cases, such as yacht racing, where teams compete in vessels of their own design, with financial sport from commercial sponsors. In the case of Olympic kayaking, there is low financial incentive to win and as a result financial support is limited. Consequently, much of the existing nautical based CFD results, may not necessarily be suitable for application, at kayaking’s unique set of conditions.

2.2. CFD

Computational Fluid Dynamics, commonly abbreviated to CFD, is a technique that makes use of parallel computer processing, to generate and solve large volumes of simultaneous fluid dynamics equations. Over time the number of cores available, on a processer has increased dramatically, making CFD work more accessible to businesses and researchers. Furthermore, modern software packages make it far simpler to create simulations, without extensive experience. The development of CFD over time can be seen by its increased involvement in competitive sports, including a variety of ball sports, water-based sports, and motorsports, where in all cases objects move at high velocities relative to the present fluids. CFD analysis can improve our understanding of how fluid dynamics effects these objects, giving a competitive advantage over others.

An article produced by R. Keith Hanna (2012), CFD in Sport – a Retrospective, outlines major improvements throughout the sporting industry, as a result of improvements to CFD analysis, between 1992, when several well-known tools such as Fluent, CFX, Star-CD and FiDAP were introduced and 2012. Whilst the accessibility of both CAD and CFD programs was a huge factor in introducing CFD to new sports, the paper largely accredits the continued success of CFD to the constant growth of available hardware. Moore's law states that "the number of transistors on an integrated circuit doubles every 2 years," (Intel 2023), Hanna (2012) suggests the same is true of the available computational processing units, CPU, and random-access memory, RAM. As a result, the mesh size of simulation was able to double roughly every 18 months, in the specified period.

2.2.1. CFD in Sports

In applications which had large enough supporting budgets, for example Formula 1, it is common now for teams to use large datacentres containing over 1000 CPUs to complete simulations. Formula 1 competition is inherently flawed as teams fully develop their own cars, there success in competition is largely dependent on the available budget and not only skill. (Barreto 2020) The introduction of CFD only increased this issue and as a result, post Hannas's article, the governing body of the Formula 1, the FIA has begun placing limitations on the amount of CFD, teams can complete in a season. The restrictions currently limit teams to 40 CFD runs per week, and after the rule changes in 2021, this amount is now scaled based on each teams' previous championship standings.

Hanna (2012) predicted that despite potential rule changes, creative teams would find a way around the rules, to complete more complex analysis such as transient overtaking simulations. In the decade since Hanna's article overtaking simulations have begun to emerge, resulting in rule changes to eliminate the use of barge boards on the cars. These are devices designed to push turbulent air horizontally away from the car, reducing the downforce on overtaking cars, which presents safety concerns. Similar concerns are often now used by teams as a loophole to apply for more CFD testing time.

Compared to Formula 1 the aerodynamics present in ball sports, such as football, basketball, or golf, may seem relatively simple, however small changes in the geometry of the ball can have a significant effect on the various techniques used in different sports. To better understand how ball geometry effects aerodynamics, researchers from the Western Michigan University (Pouya Jalilian et al. 2014), created accurate meshes of three ball types, a soccer ball, volleyball and baseball, and ran simulations at various Reynolds numbers and spin rates. The testing found that the larger soccer ball and volleyball were the most similar, both balls at Reynolds numbers above 200,000 showed that an increased spin rate greatly increased the drag forces experience by the ball. However, this also increased the pressure differential on the ball, creating lateral forces allowing the balls trajectory to curve. The spin rate on the baseball was also shown to have similar curving effects, as the other balls, however without spin rate substantially increasing drag. This allows baseball pitchers to curve pitches at far greater speeds than soccer players can curve shots.

(Hanna 2012) Given our understanding of the effect that factors such as wind can have on sports, it is common now to see CFD analysis performed on outdoor stadium and indoor sports centres. The analysis is required to provide the venues with enough ventilation for both athletes and spectators, whilst ensuring that the sources of ventilation cannot negatively affect the dynamics at play.

Generally, a ball is the most common projectile for sports throughout history, however, there has been a recent rise in popularity of disk-based sports, such as disk golf and ultimate frisbee. Frisbees come in several distinctive styles such as the parametric and the floater disc, both of which bear a resemblance to the classical discus, however all three disc are thrown differently, based on the varying aerodynamic effects that they generate. Researchers at the Sheffield Hallam University, (Lukes et al. 2014), have begun using CFD testing on Frisbees, using ANSYS Fluent, with the goal of better understanding how the geometry of the discs effects flow. There initial works are focused on two discs. Firstly, the standard parametric discs, commonly known as the frisbee, was analysed using CFD to validate potential solvers and meshing methods against existing experimental data, finding that the k-ϵ model was the best suited for disc analysis.

The focus of their work then switches to the more complex floater disc, which is shaped more like a ring, containing a central hole. They then validated the results of their flow by comparing it against the works of other PhD students, (Jonathan R. Potts & William J. Crowther 2000), who had completed wind tunnel flow visualization to understand the unique phenomena. In both studies it was observed that the flow is pulled down through the centre of the disc creating a swirling motion around the edge. Presumably by pulling air down below the disc, a low-pressure region forms above it, generating a lift force. The researchers believe that more testing needs to occur at a variety of flow velocities, disc rotational speeds and angles of attack to form a definitive theory.

2.2.2. CFD in Aquatics and Nautical Applications

Naturally in aquatic and nautical sports, athletes and their equipment are in constant interaction with the water, and hence understanding the fluid dynamics present can contribute a huge competitive advantage. One of the most prominent examples of this is the LZR racing swimsuit. (Hanna 2012) This suit was developed by Speedo, who contributed many financial resources to the suit's development, mainly to use the ANSYS Fluent CFD software. The suit was released in 2008 and was predicted to reduce the overall passive drag of a swimmer by 5%, allowing the wearers to break over 70 world records at the Olympics. Despite full body suits like the LZR being banned for modern Olympic swimming, the technology can still be seen in other sports such as skiing or bob sledding, where the aerodynamic drag experienced by an athlete is highly impactful on performance.

Improvement in such a large magnitude, is only possible in CFD studies with large investments in funding, because of this yacht racing is one of the most common applications of CFD, in the nautical space. Initial analysis in the space began with drag reduction however, studies quickly found that the weight of a vessel was a large contributing factor to drag. (Gomes et al. 2018) This is because the drag of a nautical vessel is mostly caused by the hydrodynamic forces and not the aerodynamic forces, therefore drag can be reduced by reducing the weight in a vessel and raising it out of the water, so that a larger proportion of the hull interacts with the air and not the water. Lifting the boat can be accomplished in several ways, and yachting teams have since developed several methods of generating lift.

The most predominant way of generating lift on a nautical vessel, is with a hydrofoil. Similarly to an aerofoil, a hydrofoil generates lift through the shape of its cross section, which has differing perimeter lengths above and below the centreline. These differing lengths create different velocities as fluid travels over them, creating a pressure differential, which causes lift on the vessel. (Shen et al. 2022) Research shows that at perfect conditions the total drag reduction on a planning boat, using a hydrofoil can be as great as 30.74%. The boat simulated was not however a traditional racing yacht, and therefore a large amount of the hull remains in the water. Therefore, the drag reduction effects in yacht racing could potentially be even greater.

The large drag reduction advantages of hydro foiling boats are not common to see on a recreational vehicle, due to safety concerns. For nautical vehicles hydrodynamics are not only a factor in the top speed of a vessel, but they also affect a vessels ability to turn. For the vessel to create a turning force it needs to impart an equal and opposite force onto something, and given the much greater density of water, when compared to air, contact between the hull and the water, greatly increases the turning forces created.

Despite safety concerns it is however unavoidable that sports technologies will continue to trickle down from CFD into the commercial space. Students at Ghent University, (Bagué et al. 2021) Belgium have been undertaking CFD research to develop methods of analysing the stability of hydro foiling vessels. Development was initially focused on analysing a single vessel, called the "Goodall Design Foiling Viper." This vessel is capable of fully raising itself above the water at sufficient speeds, however, consists of a unique design that promises to increase stability for users. This is accomplished using a combination of both, Z shaped dagger boards, to provide stability at the centre of gravity, and T shaped rudders, to provide both, lift at the rear of the vessel, and stabilise the vessel from rotating backwards, all whilst allowing the vessel to be steered. After conducting CFD analysis on the vessels, the results are incorporated into an analytical model, to give vessels a stability score. This is more complex than a simple number, and is represented by several complex eigen vectors, representing, damping, heave, pitch, and wobbling. To confirm the validity of the analysis it was compared to experimental results from sea trials of the vessel. To accelerate the development of the model, the researchers have made the code open source, it is called typhoon and is available on the Ghent university website.

The dynamics of vessels are not only limited to the forces on the hull. Dynamic forces can be affected by a variety of sources including, forces of propulsion, forces imposed by the crew and stability changes by cargo. Despite dynamic performance not being a huge contributing factor to the success of Fishing Boat, the variations in cargo are highly significant to the dynamic stability of the vessel. The vessel contains both large fuel tanks and fish tanks, which store fluids that can act unpredictably, furthermore both crew, and solid cargo, including bait and fishing gear, regularly move around the deck, all this affects dynamics by changing the vessels centre of gravity. The additional loads imposed using cranes and winches, contribute to fishing boats being generally unstable vessels. (Iqbal et al. 2024) CFD can be a useful tool to model the effects of parametric roll caused by unpredictable sea conditions. Through transient simulation the dynamics of parametric roll can be simulated, with the inclusion of potentially unstable fluids housed in the vessel. CFD studies have found that the maximum amplitude of the parametric roll is up to 16.33% higher than that suggested by existing literature, suggesting that higher standards of safety are required to prevent future incidents of roll over.

2.2.3. CFD in Kayaking

To ensure that CFD is an effective tool for analysing any sport, it is important to first validate the general suitability of the technology, by comparison of results against alternate methods. Generally experimental analysis is best used for validation, as it has considerably fewer technological limitations, mainly that of measuring techniques and equipment, which can be accounted for, with a specified margin of error. For kayaks, and other nautical vessels, testing is typically completed by using a towing tank. Towing tanks are an indoor controlled body of water and are usually quite long and slender. A variety of rail systems can be employed to suspend a vessel into the body of water and test it at various velocities.

In 2010 (Georgios D. Tzabirus et al.), an experimental study was undertaken by the National Technical University of Athens, at the Laboratory of Ship and Marine Hydrodynamics. The experiments undertaken involved the testing of an Olympic K-1 kayak, at a variety of speeds and conditions, in a towing tank. The goal of the study was to use the results to validate the applicability of the Reynolds Averaged Navier Stokes solver, for use in kayak testing, by using it to generate the same set of results as the experimental tests. The research found that the solver was reasonably accurate, provided the kayaks velocity is limited to realistic race speeds, and testing occurs at calm water conditions. Rocha Barros (2015), found that generally CFD modelling tends to underestimate the total drag as fluid velocity increases, which was found to occur at speeds as low as 3.69 m/s even at calm ambient conditions.

Towing tank analysis has several key limitations, all determined by the size of the tank, which include, vessel size and speed, as well as the duration of sustained consistent test conditions. Similarly to with aerodynamic wind tunnel testing, a common method to make testing more accessible, is to test with scaled models, which can reduce both, the initial investment cost in the testing facility and the continued cost of model manufacturing. Barber (2018), conducted research using a 1:6 model of a kayak in a wind tunnel, to determine the aerodynamic drag on a kayaker. Assuming the model is as valid as a hydrodynamic model, CFD analysis should be similarly validated against these findings, not only to determine which model produces more accurate results, but to compare the effectiveness of each technique, relative to the required time investment. Should the model be inaccurate, however time and cost effective, it may still be applicable as a design tool, allowing designers to effectively reduce the time investment in initial design iterations, on poorly optimised hulls.

2.3. Kayak Origins and Development

Since they were initially developed thousands of years ago, the size, shape and materials used to make kayaks have changed greatly. These changes can occur for several reasons, such as a change in how we use them, development and design improvements over generations and general improvements in technology, often from other fields. Understanding how kayak design has changed throughout time and why, is a key step to understanding the performance characteristics of modern kayaks and their limitations.

2.3.1. Kayak Design

The first evidence of kayak use is believed to have been from approximately 5,000 years ago, where the Inuit and Aleut people used them to traverse the water in Artic North America. (Pladdles 2017) These kayaks could be as long as 18 metres, as their main purpose was to transport multiple passengers and cargo. Kayak designs however ultimately became much shorter when their inventors realized how effective they were at sneaking up on prey in the water. These smaller sized kayaks are a lot more similar, in general shape and overall size, to something you might buy today. The smaller size, reduced weight and easier manoeuvrability make them more useful for many solo hobbyists, who can use them on their own to explore, exercise and fish. (Castillo 2022)

(Day c. 2024) Modern kayak designs still vary a lot, based on the use case of the vessel. Fishing kayaks feature a wide cross section, which provides the kayak with much greater stability, space for a seat and the ability to stand on them. These designs however are relatively slow, likely due to higher drag because of an increased cross section. An opposite example to this is a whitewater kayak, these are designed for high manoeuvrability and are shorter than the average kayak. The overall shape of the kayak is designed to ride on top of waves in river rapids and features a small seating area enclosed by a waterproof skirt.

The driving force behind many improvements in the nautical area is competition, in the case of kayaking the main competition is the Olympic games. (Pladdles 2017) The sport of kayaking was first introduced to the Olympic games in 1936 at the Berlin Olympics. (Robinson, Holt & Pelham 2002) Correlations in race performance can be seen in Olympic race times, after the introduction of several major design styles, starting with the V-form at the 1952 games, then the diamond shape at the 1960 games, followed by the delta shape at the 1972 games, and finally most recently the change to an eagle shaped design at the 2000 games.

2.3.2. Kayak Manufacturing

Whilst kayak design choices are often dictated by their intended use case, much of the major design changes throughout history are more closely correlated with the introduction of new materials and manufacturing techniques. (Pladdles 2017) The original kayaks designed by the Inuit and Aleut people, were primarily constructed from animal bones, with animal skins stretched over them. The quality and shape of these kayaks' designs were limited largely by materials, these kayaks were extremely light however equally fragile. Seal bladders were often filled with air and attached to the kayak to increase the vessels buoyancy, a practice now materially limited by animal rights legislation, however alternative styles of inflatable and multihull design achieve the same purpose.

(Outfitters c. 2024) The first major material change for kayaks was the change to using wood. Compared to using animal bones, a wooden kayak provided far greater rigidity and durability to the kayaks hull, at the expense of increase weight, which reduces the overall buoyancy of the kayak. The use of metal as a material offers the same strengths and weaknesses again over wood. As a compromise between weight and durability, it was therefore not uncommon to see kayaks be constructed of a wooden or steel frame and rapped in a flexible skin, this style is still a common method of constructing foldable lightweight kayaks.

The second major material change for kayaks was the introduction of plastics. Polyethylene is a popular cheap material for kayak manufacturers, and is easy to manufacture, often used to make entry level kayaks. Once again weight is the main material limitation. Whilst more expensive than roto-moulding plastic, thermoforming is a common manufacturing technique in which thin plastic sheets are heated and wrapped around a mould. The plastics in this process can often be hybrids and overall, the process results in a lighter kayak design whilst maintaining or increasing the strength of the kayak.

Composite materials offer many advantages over plastics, mainly increased strength to weight ratio and hull rigidity. Most composite materials consist of some fibrous material applied in layers and bonded with resin. The manufacturing process is therefore similar to thermoforming, allowing the same designs to be produced however less material is required to produce the same strength levels. It is also worth noting that composite materials can often be repaired by adding additional material to damaged areas, however this may compromise the overall surface finish of the hull. The most common composite material used in kayaking today is fibreglass, however there are constantly new additions being produced in the composite space and therefore kayak materials may continue to change for years to come.

2.4. Kayak Performance

To ensure that a CFD model can produce applicable results, a key step is identifying what factors affect real-world performance. In the context of this research the major focus is kayak performance, therefore the model should measure as many key performance indicators as possible. The major factors of kayak performance include, stroke rate, the profile of the stroke, drag, the level of the kayak relative to the free surface and the ambient conditions surrounding the kayak.

2.4.1. Stroke Performance

The propulsion of the kayak is ultimately determined by the stroke of the paddle. The force imparted on the water, as it is displaced by the paddle, contributes an equal and opposite reaction to the kayak propelling it forward. The amount of work achieved by a kayak stroke can therefore be increased by increasing the overall length of the stroke. Naturally the power generated by the athlete is the product of, the work generated per stroke and the frequency each stroke. In a similar past literature review, (McDonnell, Hume & Nolte 2013) it is determined that both stroke rate and length are the most important factors in the overall speed of the kayak, however due to the geometry of the human body the stroke length is ultimately limited. The review ultimately determines that the best way to increase performance for a kayaker, is to maintain strokes at the maximum possible length, and then complete them at the highest possible frequency, rather than attempting to complete shorter strokes at a higher rate.

2.4.2. Stroke Modelling

In more commonly simulated areas such as yacht sailing, propulsion is achieved using sails. As the sails are positioned sufficiently high above the free surface of the water, their effect on the drag experienced by the hull is negligible, this however is not the case for a kayak. To produce a propulsion force, the kayaker must impart a force on the water surrounding them, this changes the profile of the flow at the free surface surrounding the kayak significantly. Research shows (Morgoch, Galipeau & Tullis 2016) that the impact of the paddle, on the profile of the water, is significant not only because of the total volume of fluid displaced, but also because the paddle creates vortices along its edges. This occurs because as fluid passes over the edge of the paddle, it is pulled around behind the paddle, to fill the volume behind. These vortices create a major disruption to the streamline of the flow and are larger and more significant near the paddles tip, creating larger disruptions below the free surface, far beyond the kayak's hull.

Modelling the effects of a moving paddle, would require the CFD model to be transient, significantly increasing computational time. An alternative method is outlined by Bank's (2014) research, in which a transient model is produced of the paddle passing through an equivalent body of water. Using this model, the net change in velocity can be determined and applied to the final flow profile around the kayak. This process is reported as adding only 8% extra computational time, to the existing kayak model Banks used.

Bank's paddle model is useful in identifying the effect of paddling forces on the velocity profile of a steady state flow, however in reality the velocity of a kayak is never steady state. The propulsion from a kayak paddle, assuming a constant stroke rate, is cyclic at a frequency consistent with the stroke rate. It can be seen experimentally, (LeroyerDuvigeau, et al. 2016) by attaching several GPS accelerometers to a kayak, that the velocity of the kayak oscillates above and below the average velocity of the kayak. This occurs cyclically with a frequency consistent to the stroke rate of the kayaker. Therefore, to accurately model the kayak, a transient model would need to be used to model one full cycle of a kayaker's stroke. Experimental data (LeroyerDuvigeau, et al. 2016) could be used to define an average cycle of inlet velocities relative to the kayak as a boundary condition.

Another limitation of the accuracy of a paddles stroke is the deflection of the paddle. Cheap consumer paddles or flippers are often more flexible than professional equipment. The flexible equipment reduces the physical strain placed on the user, making the product more widely accessible. The flexibility of the paddle also reduces the force that a user can exert on the water to propel themselves, and thus the impacts on the flow around them. Further works by Leroyer, (2016) show that modelling the flex of the oar through a stroke is beneficial to reproducing experimental results.

Whilst to impart more force on the water, a kayaker needs to exert more force with a given paddle stroke, changes to the paddles stiffness and ergonomics can also be useful at increasing the force output of a kayaker. CFD research by Harrison, Cleary and Cohen (2019), uses the results of CFD models and biometric models to determine the amount of force and torque on a kayakers joints during a complete stroke. This analysis could allow the researchers to identify paddle materials, designs and techniques that allow athletes to create power more efficiently throughout a race.

2.4.3. Kayak Drag

Kayak drag is most effected by two major components, pressure drag and frictional drag. It is also important to consider the ambient conditions surrounding the kayak, such as wind and water, speed, and direction. These conditions effect how the fluids interact with the kayak, above and below the water as well as at the surface. Another important consideration is the kayaks wake, which can also be affected by ambient conditions as well as proximity to other vessels and the edge of the body of water.

When a vessels hull, forces water out of its path an equal and opposing force is applied to the kayak, this force is commonly referred to as pressure drag. It can be seen by the wake of a vessel, which extends beyond the hull, that marine vessels are required to displace more water than simply the volume of the hull. The shape of the hull is particularly important to minimising drag, by creating a slenderer hull profile a minimal amount of flow separation is required, reducing the amount of water displaced, the force required to do so and therefore the pressure drag on the hull.

The forces created by the interaction between the water and the hull are also a major factor in the friction drag experienced by the kayak. Water is forced into the hull during motion, these forces must be overcome by the water so that it can overcome imperfections on the surface of the hull. The opposite force imposed on the hull is commonly known as frictional drag. As frictional drag is proportional to the force acting normal to the hull of a vessel, it is linked to the pressure drag. Therefore, changes in the shape of the kayaks hull that reduce pressure drag may also be effective at reducing frictional drag. The most common method for reducing frictional drag would, however, be to improve the surface finish of the hull, reducing the frequency and size of imperfections and the required force to overcome them.

Generally, the magnitude of drag on a vessel's hull due to water, is far higher than that of the air. Therefore, wind speed may seem like a relatively small contributing factor to the overall drag experienced by a vessel, however, can have a huge effect on the free surface of a body of water. In specific cases such as a large storm or when using a kayak, the magnitude of the turbulence at the free surface can be quite large relative to the size of a vessel and can therefore have a large effect on the overall drag experienced. (Wüthrich, Shi & Chanson 2021) Experimental research can be carried out using breaking bores which are filmed using high speed video. This research is generally undertaken for the purpose of hydrology, where researchers wish to better understand the unpredictable nature of water, during a large weather event, such as a tsunami. The research creates useful kinematic data, which has been used to further our understanding of free surface effects.

The wake of a vessel is generated as water is pushed out of its path, and therefore like pressure drag the magnitude of the wake, is affected by how slender the profile of the kayak is. The wake effect can be observed far from the kayak itself, and as a result there exists potential for a kayak to be affected by the wakes of other objects, or by the reflection of wakes off these objects. To test the wake effects of vessels the Pprime Institute of the University of Poitiers, France (Caplier et al. 2019) have developed a towing tank to experimentally test the wake effects of vessels. The force required to reflect the wake back off the bank of a river or canal can be considerable enough to cause erosion over time. Whilst erosion research was the primary reason for developing the towing tank initially, it has been used for several other studies, including measuring changes in the free surface level, on either side of a vessel, where the vessels cross section is large enough relative to a channel's width, to prevent displaced water from flowing around the vessel.

2.4.4. Kayak Drag Reduction

Another literature review was conducted by Mohammad and Majid (2015), to investigate a variety of different modern drag reduction methods, with a primary focus on larger vessels such as cargo ships. The review therefore often considers, wave making resistance and fuel economy, which are factors that are less applicable to flat water kayak racing. The review is primarily broken down into three sections, hull optimisation, air lubrication and fouling and coating.

As discussed previously one way to reduce the pressure drag on a hull is to make it slenderer, however for large vessels this will result in a reduction in the available deck area. For certain applications, such as passenger vessels, a reduction in deck area is not possible without compromising other aspects of the vessel, therefore in such cases it is common to see a catamaran or a swath type vessel. These vessels use two separate hulls positioned at either side, which allows them to maintain the same deck width and stability with reduced drag. By using two separate more square hulls the ratio between volume and wetted surface area is increased, meaning that below the water line the same volume required for buoyancy can be achieved, at a reduced surface area.

Another strategy to reduce the wetted surface area of the hull is to reduce the required buoyancy and therefore hull volume. This is often achieved in yachting by introducing a keel, a fin like device capable of generating a substantial amount of lift at high speed. As the lift increases, the buoyant force required by the hull reduces. The hull will therefore begin to rise above the water, until the remaining volume in the water, has reduced to generate only the remaining required buoyancy. As this occurs the wetted surface area will also reduce, resulting in less overall drag on the vessels hull.

Whilst not commercially available, the theory behind air lubrication, created several interesting drag reduction techniques. Mohammad and Majid (2015) summarise the current research into three techniques, micro layer bubble reduction, air layer drag reduction and partial cavity drag reduction.

Micro bubble reduction involves creating a layer of bubbles that flow over the submerged portion of a vessels hull. The bubbles cover the turbulent boundary layer usually present near the hull; this layer is extremely important in the creation of friction drag. The aerodynamic drag created is far less significant than the hydrodynamic drag otherwise created by the water. There is also the potential at low speed for the bubbles to create a buoyancy effect, which could reduce the surface area, of the now partially wetted surface of the vessel. Air-layer drag reduction is a similar technique, where air is injected to form a complete, however thinner, layer of air over the vessels hull. With this technique it is important to consider that an air layer over the hull surface is not a replacement for a suitable surface finish, as the air layer must also interact with the vessels hull. Partial cavities drag reduction is like air layer drag reduction, however, often creates multiple small air cavities rather than one continuous layer. In comparison partial cavity drag reduction is initially more expensive, often requiring a unique hull design or extensive modifications to an existing one. The technology does however show potential to provide substantial efficiency gains relative to the power requirements of the fans used to generate the cavities.

Fouling's and coatings are likely the most applicable drag reduction technique, from Mohammed and Majid (2015) literature review, to flat water kayak racing, however many of the potential causes of fouling are vessel specific and many vary based on manufacturing. Potential causes of fouling may include welding or other assembly techniques, damage and wear, material imperfections, and over time may increase due to corrosion or accumulation of biological matter, such as algae. Wang et al, (2018) conducted experimentation to investigate how fouling control coatings could be used to reduce the frictional drag on a vessels hull. Four different coatings were tested, broken down into two categories, fouling release and antifouling coatings. Generally, the fouling release coating resulted in around 5% less drag, however the results can vary, primarily at differing velocities. One potential concern of the coating was how their effectiveness would change based on levels of water absorption. Overall, the effects of water absorption were found to be mostly insignificant to performance, except for in some causes with antifouling coating, in which it resulted in improvements. Wang et al. (2018) also investigated the effects of weld seem height on drag. It was found that weld seem height was extremely significant to the drag forces on the vessel, primarily at speeds over 15 knots. Based on the results a maximum weld seem height of 5 mm was recommended.

3. Methodology

3.1. Overview

Before proceeding with the analysis, it was important to create a plan capable of meeting the object of this research, which is to create a model that can solve for drag properties on a kayak and kayaker throughout the range of reasonably ambient conditions, that may be present in an Olympic flat water kayaking race. This can be achieved by using CFD software to solve the flow of the fluids, both air and water, across a range of data points within a relevant simulated volume, containing a three-dimensional model, to represent the geometry of both, a kayak, and a kayaker.

Available resources are generally the major limitation in research methodology, as a student the most accessible CFD software is ANSYS. The fluent solver is a part of the ANSYS software package and is a suitable choice for the fluid-based simulations required for this research. The effectiveness of this software package is however limited by the hardware available. To more effectively utilize fluent, access was granted to UniSQ's High performance computing cluster, known as Fawkes. This HPC has over 3000 computational cores and over 24 Tb of memory, which can be utilised to decrease computational time, solve large domains and solve with finer mesh sizes. For this research, the HPC was accessed using Strudel, a windows VNC software, which has been limited to 64 cores and 512 Gb of memory.

3.2. Free Surface Modelling

The drag force experienced by a kayak are produced through interaction between the kayak and the fluids surrounding it. These fluids do however also interact with each other, in fluid dynamics this is commonly referred to as a free surface. Interactions at this surface may cause some fluid mixing, this may create some ripples or even waves given enough energy is present. Free surface interactions occur in a comparable way to how walls create boundary layers, due to friction with the boundary surface. Ideally for a multiphase flow each fluid treats the other like a boundary surface, however as flows become more turbulent, the free surface effects become less predictable.

In the case of flat-water kayaking, it is highly unlikely to observe waves, however as the kayak floats on the free surface, interactions between the fluids will certainly affect the flow around the kayak and subsequently the drag forces present. The accuracy of the free surface modelling is therefore crucial to the accuracy of the overall kayaking model and time was therefore initially allocated to modelling the free surface alone.

This began by attempting a simulation of a free surface using standard multiphase VOF settings in ANSYS Fluent. This was done to gain an understanding of the limitations of the software and an understanding of what inputs the software requires from the user to accurately simulate a flat body of water. The initial simulation volume was of a rectangular prism with dimensions of, 10m x 10m x 50m, initially spliced into two parts. This also created two separate inlets, an air inlet for the top half and a water inlet for the bottom half. It was assumed that generally the wind velocity would be of higher magnitude and the water current present, therefore the air and water inlet velocities were specified to be 5 m/s and 1 m/s, respectively, both in the direction normal to the inlet. A mesh is then generated without any refinement and a maximum element size of 0.5m was used.

The solver is set to transient, therefore gravity must be defined and has been assumed as -9.81 m/s^2 for this analysis. Transient solvers generally require a significantly small step size to accurately solve a simulation, in this case 0.01 s was used. For a multiphase solver, a surface tension coefficient is also required, as this value varies due to temperature, standard temperature pressure has been assumed, making the surface tension coefficient equal to 0.072 N/m. Instruments (c. 2024)

Standard initialization in ANSYS applies an initial set of property values to all nodes in the volume, however in the case of a multiphase simulation different properties need to be applied to areas containing each phase. This can be achieved by applying a patch, this allows you to apply a separate set of fluid properties from a second phase to a named section of the volume. It is generally considered good practice to specify the less dense fluid as the primary phase. In this case the primary phase would therefore be air, and the secondary phase, which was patched into the standard initialisation, will be water.

To check if the simulation produced an appropriate free surface, a phase contour plot was generated. This plot displays the phase present at points across the volume using colour, where red represents the primary phase, in this case air, and blue represents the secondary phase, in this case water. The colours in between represent various amounts of mixing, and therefore it is expected that a vertical cross section of the volume should show a consistent colour gradient from red, above the free surface, to blue, below the free surface. Figure 1 shows a contour of the initially attempted simulation, it can be seen from this that at the inlet, on the left side of the contour, the flow enters at the correct heights, however the flow almost immediately drops. At this stage it was believed that this occurred as both inlets have an equal area, but differing velocities and therefore volumetric flow rates. As the two flows move towards the outlet the flow velocities begin to equalise, however because the flow rates across the inlet and outlets must remain constant. the area each fluid occupies at the outlet must change.

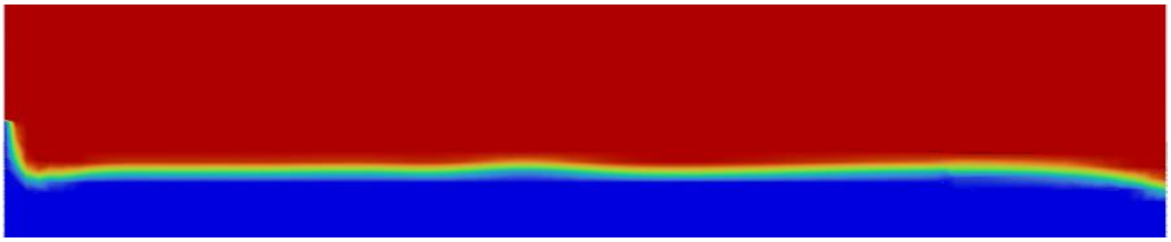

Figure 1 - Phase Contour Default settings.

To fix the free surface model, multiple mesh refinement techniques were attempted including, generally reducing the element size and introducing an element sizing method. The element sizing method in this case was used to specify a different element size at the free surface, in this case within 25cm. An automatic mesh adaptation was also added, using Fluent's predefined criteria for multiphase, volume of a fluid simulations. The flow showed a noticeable improvement now maintaining a free surface for most of the volume, as seen in Figure 2. The simulation also converged with far fewer iterations at each timestep, therefore these additional mesh refinement techniques continued to be used throughout the following research.

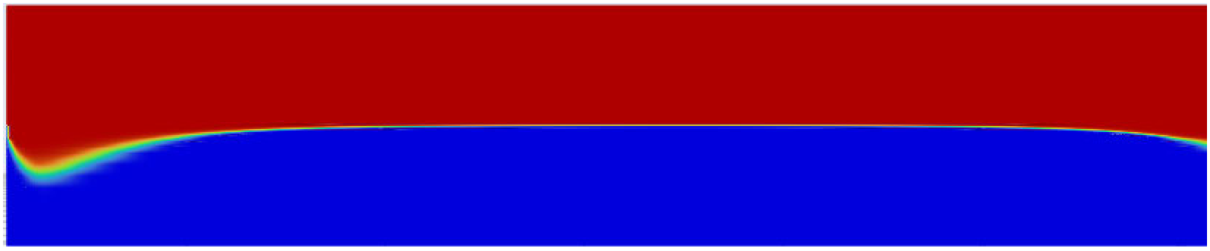

Figure 2 - Phase Contour with mesh refinement.

It became apparent that to achieve the perfect free surface desired for this research that, the location of the free surface would need to be defined explicitly. This was achieved by applying a VOF Sub-Model, called Open Channel flow, which allows the free surface level to be specified at the outlet. Unlike in the original trial as shown in Figure 1, the outlet no longer achieves equal velocities. Instead, the flow slowly transitions from the inlet profile to the outlet profile. As these two profiles are the same in this research and because there is currently no kayak to obstruct the profile throughout the volume, it remains constant. This is the desired outcome of the model and will be used throughout the following research.

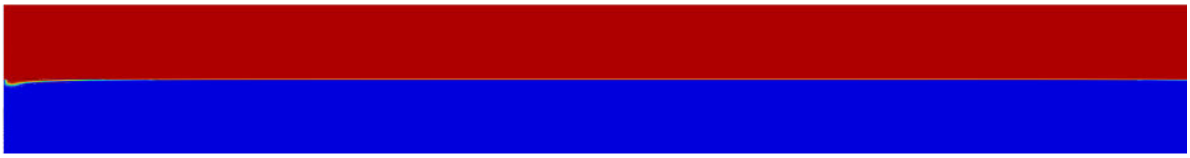

Figure 3 - Open channel flow.

3.3. Kayak Modelling

In any drag study, the trend of the data, against fluid velocity, will always follow a generally similar trend as drag is a function of velocity squared, (Benson c. 2024) as shown in Equation 1. As density is a set value for the fluids in our simulation, the result will therefore be largely dependent on the kayak size, and shape, as these attributes effect cross sectional area and drag coefficient respectively. To produce accurate and applicable results, the modelling phase of the research is therefore crucial.

$$D = \frac{C_d \rho V^2 A}{2}$$

Equation 1

Due to the limited resources of this research and the premium price associated with specialist kayaking equipment, it was not feasible to obtain even a single seater kayak, known as a k1, that would be representative of what Olympic competitors use. Instead through a personal connection, a single seated fishing kayak was available for measuring, as shown in Figure 4. Fishing kayaks such as this one differ from k1's in several notable ways, mainly the overall shape or profile. These kayaks are shaped differently to a sprint kayak as they are designed for a different purpose, fishing, which has different desirable performance criteria to flat water sprint racing.

Figure 4 - Measured Kayak

Generally, a sprint kayak is designed to be long and slender, this both reduces the overall pressure drag, which enables kayakers maintain higher speeds over extended periods, and increases the second moment of area about the axis normal to the surface of the water, which reduces the torque effect of unequal rowing forces on the rotational velocity of the kayak.

Fishing kayaks are generally wider and shorter by comparison, this generally makes the kayak more manoeuvrable, at the compromise of lower speed. The extra width increases the kayaks second moment of area about the longitudinal axis on the kayak (axis between the tips on the kayak), increasing the kayaks resistance to lateral rotations, caused for example by fishing rods, in some cases this even makes the kayak suitable to stand on. This style of kayak may also feature grooves in the hull, these are designed to increase the lateral pressure drag on the kayak, so that the kayak can change direction effectively even at lower speeds where friction drag is relatively low.

Using the fishing kayak does therefore limit the accuracy of the model for use in analysing the performance of an Olympic sprint kayak race. The accuracy could be improved by assuming dimensions of the kayak that generate a more appropriate shape; however, this method would not be as precise. The decision was made to measure the geometry of the fishing kayak as the research findings would therefore be precise and applicable to a real kayak, however not a k1 style of kayak. Some compromises were made to the geometry, such as removing the longitudinal grooves in the kayaks hull or the detail of the kayak's deck. Generally, this was done to simplify the geometry of the model, as these features are complex and hard to accurately measure. Whilst this will reduce the precision of the model as a fishing kayak, this may result in the model producing results that are slightly more representative of a k1 style kayak, and therefore this should be an appropriate compromise for this study.

Before measuring an object in person, if the intent is to model the object, it is important to first consider what techniques are appropriate and available. In the case of most objects that interact with a fluid the surface of the object is generally the most critical, as it interacts with the fluid directly. The cross section of the objects surface generally experiences a gradual change in the direction normal to the flow, as to not cause turbulent separations of a fluid. Most CAD software have a tool for creating geometries such as this, commonly referred to as loft. The loft tool allows the user to generate a continuous geometry between a discrete number of cross sections, provided these cross sections contain the same number of vertices. For this research PTC Creo Parametric 11.0 Student Edition was used to generate CAD, this software offers a tool called blend, which has the same functionality as loft does in other CAD software.

To measure the kayak with the intent to use the blend tool, the geometry first needs to be divided into a discrete number of cross sections. A total of ten cross sections were chosen at planes normal to the kayak's length, including one cross section at either tip of the kayak. Given that the kayaks total length is 2.7m the cross sections were spaced evenly at 0.3m increments, as shown in Figure 5.

Figure 5 - Kayak Cross Section Distribution

At each cross section four points are measured, the first is at the centreline of the kayak, the second is at the centreline of the concave curve in the hull, the third is along the edge of the kayak hull, and the fourth is at the edge of the kayak deck. It was assumed that the kayak is symmetrical across its width. Approximate continuous lines for these points over the kayak's length can be seen in Figure 6 marked in blue. The datum lines of these points can also be seen in Figure 6, marked in red, where the x datum is at the centreline of the kayak and the y datum is at the lowers point on the kayak.

Figure 6 - Kayak Cross Section Measurements

Each point is measured to find an x and y value relative to the datum lines, at the first five cross sections along the length of the kayak. The remaining 5 cross sections where not measured due to the assumption that the kayak is symmetrical along its length. The other assumption that was made is that the kayaks width at the deck and the hull are equal, meaning that the x value at point three and point four are always equal. In this case the x value was always measured at point three and assumed for point 4. Finally, all the y values were transformed, this was done as to effectively shift the datum plane to be located approximately at the waterline relative to the kayak. The waterline was approximated to be 200mm above the base of the kayak, through consultation with the kayak's owner. The final measurements are summarised in Table 1.

Table 1 - Cross Sectional Measurements (cm)

Point	Cross Section	1	2	3	4	5	6	7	8	9	10
1	x	0	0	0	0	0	0	0	0	0	0
	y	15	-15	-20	-20	-20	-20	-20	-20	-15	15
2	x	0	11	22	26	26	26	26	22	11	0
	y	15	1	-6	-11	-17	-17	-11	-6	1	15
3	x	0	18	30	37	40	40	37	30	18	0
	y	15	5	-5	-10	-14	-14	-10	-5	5	15
4	x	0	18	30	37	40	40	37	30	18	0
	y	15	15	15	15	15	15	15	15	15	15

When constructing the model in Creo Parametric the origin was positioned at waterline on the symmetrical centre axis of the kayak. Figure 7 shows a sketch at the fifth cross section, also mirrored to the sixth cross section later, which is typical of the sketch shape used at all the cross sections. The sketch consists of three lines mirrored across the vertical centreline, one line is an arc consisting of points one two and three. Another is a line between points three and four, this line is always vertical as the width of the kayak hull and deck have been previously assumed as equal. The final line is a horizontal line from point four to the vertical centreline, this simplified the geometry of the kayak as previously discussed, creating an artificially closed kayak deck, which is coincidently more representative of a k1 style kayak.

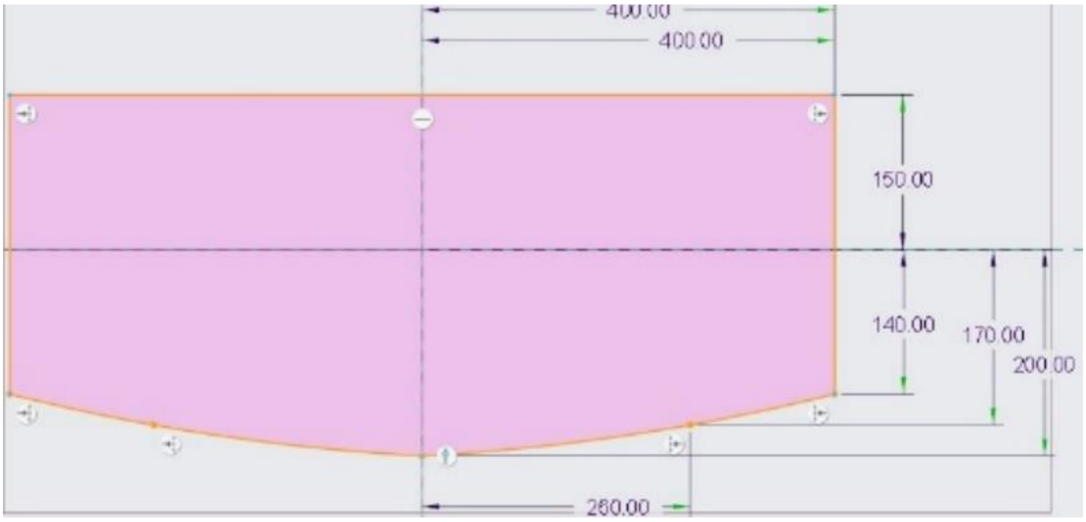

Figure 7 - Cross Section 5/6 Sketch in Creo

For the blend tool to work effectively each of the cross sections need to have a sketch with the same number of vertices, ideally in a similar distribution to the adjacent cross sections. As the first and last cross sections of the kayak are the tips, their geometry is best approximated as a point, however, to better satisfy the sketch requirements of blend, they were sketched as exceedingly small cross sections, to match the same general shape used along the kayak. The final dimensions can be seen in Figure 8.

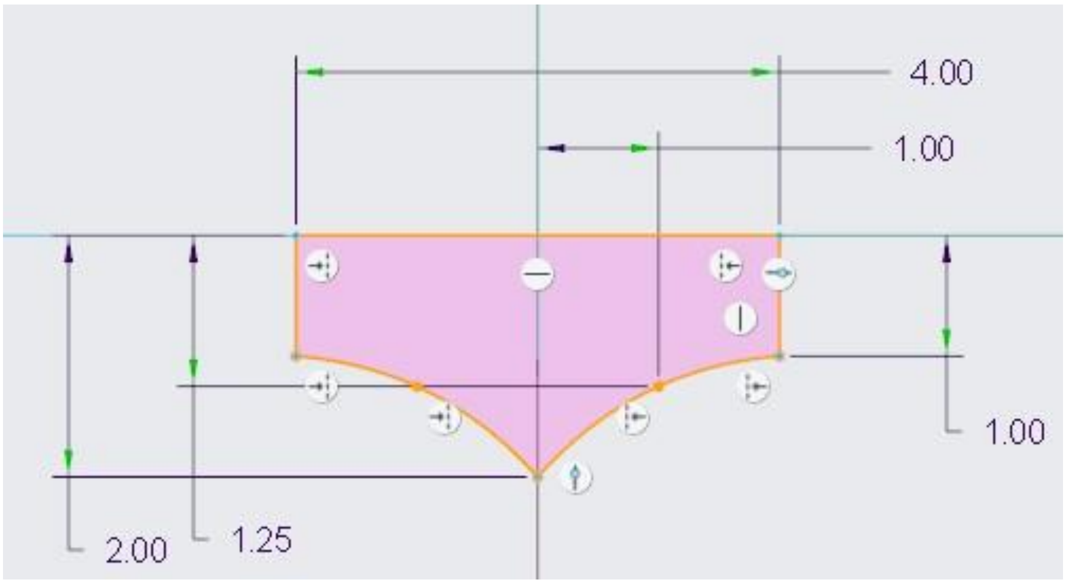

Figure 8 - Tip cross-sectional sketch in Creo.

Finally, the cross sections are blended to form the simplified geometry of the fishing kayak. Upon blending the geometry, it was noticed, that at the intersection of the lines in the cross-sectional sketches, sharp edges form along the length of the kayak. This is not representative of the kayak and may cause the model to create inaccurate turbulent flow separations in a fluid simulation. A 10mm fillet, referred to as a round in Creo Parametric, was therefore applied to each of these edges. The resulting geometry can be seen in Figure 9.

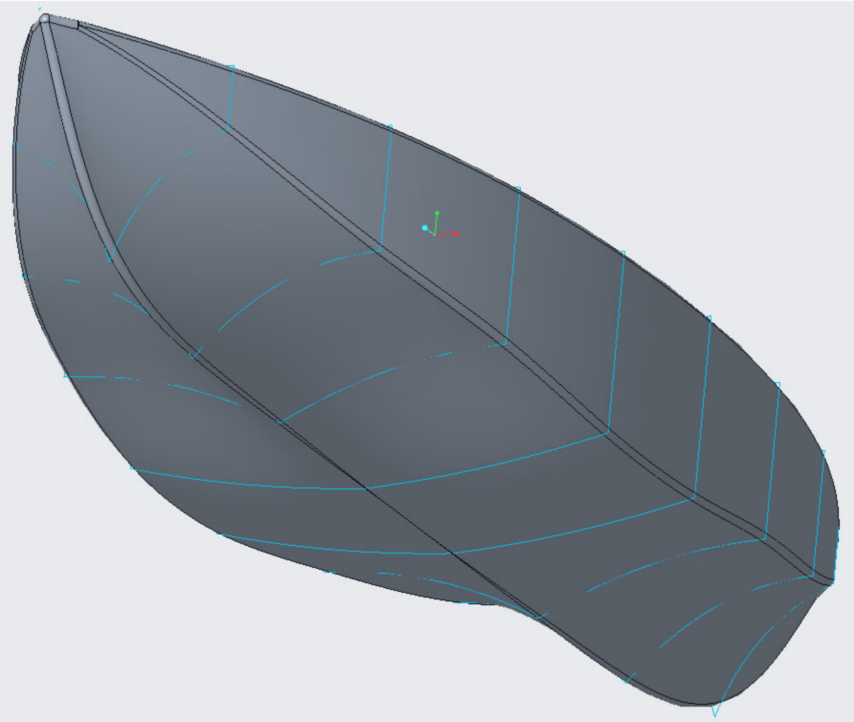

Figure 9 - Creo Blended Kayak

3.4. Kayaker Modelling

Similarly to with modelling the kayak it is first important to consider how modelling a kayaker may be achieved before proceeding. Human geometry is far more inconsistent and complex than that of a kayak, and therefore, as was done with the kayak, the geometry of the kayaker will need to be greatly simplified, before modelling. In the case of this research only the upper body head and arms needed to be modelled, and were to be represented by simpler, but similar, basic 3D geometric shapes. The dimensions of the geometry were based on the rough body dimensions of the researcher, who is not an athlete.

Creating the geometry in this way has several limitations to accuracy, mainly the accuracy of the body shape however also the accuracy of the body size. It is however crucial that some kayaker geometry is included, as the kayakers body creates a relatively large amount of the aerodynamic drag in the model. Additionally, in a flat-water kayaking event, the ambient wind conditions vary more often, relative to the waters current. Kayakers body shapes and sizes do also vary significantly based on genetic factors, and it is therefore not as crucial to invest significant time into creating a perfect kayaker model, instead the objective of modelling a kayaker, is to create a representative model, that will not significantly alter the observable drag trends between different wind conditions.

The first step in creating the kayaker's geometry was to create the torso. The torso's vertical cross section consists of an oval, of a 400mm width and a 200mm length, positioned 250mm behind the origin of the model, the symmetrical centre of the kayak, as this is the kayakers approximate seating position on the kayaks deck. The overall height of the torso is 700mm. The next step is to add a head, approximated as a vertically extruded cylinder of a 200mm diameter, and 300mm total height, positioned at the centre of the top of the torso.

The following addition is slightly more complex, which is the kayakers' arms. In this case assumptions will need to be made about not only the relevant lengths and sizes, but also the positioning. As the positioning of a kayaker's arms are not constant with time, the shape of the body and therefore the drag experienced by it is not constant, but approximately cyclic. To get a full understanding of the drag experienced by a kayaker, further research could be conducted to calculate drag at several of a kayaker's poses, spaced equally through there stroke cycle, the average of which would be a more accurate representation of the drag experienced by a kayaker throughout a race. For the purposes of this research, it is more important to determine how changes in the ambient conditions effect drag, therefore a single pose is sufficient to generate the desired results.

For simplicity, a symmetric pose was chosen, with the kayaker holding the paddle out directly in front of themself, this would represent the midpoint of the kayaker's transition from paddling on one side to the other. The arms have been created using the sweep tool in Creo Parametric. This tool is like the blend tool discussed previously in this report, as it allows the user to create a continuous section from a discrete profile. In this case one profile is used, however this profile can be swept along a continuous path, containing any number of directional changes.

The path was sketched onto a plane 600mm above the surface of the kayaks deck, it contains one bent line starting 150mm in width from the centre of the torso. The line has a total length of 600mm, starting at an angle of 60 degrees outward from the front of the kayak, bending 90 degrees inward at its midpoint. The swept profile is circular with a diameter of 100mm and is mirrored across the centreline plane of the kayak, to form the other arm.

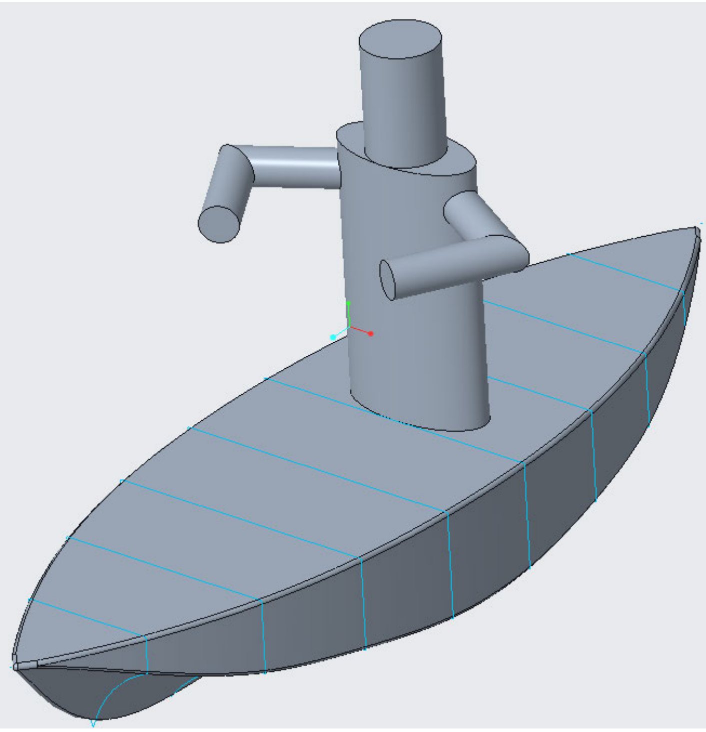

Figure 10 - Simplified Kayaker Geometry

The resultant geometry is shown in Figure 10, and similarly to the kayak geometry it initially contained many sharp edges that are not typical of a human body. The geometry was therefore rounded, at a variety of radii. The top of the head and ends of the arms were rounded by their respective diameters to form hemispheres. The arm joints were rounded at 25mm, along with the neck and shoulders. Finally, a round is applied to the base of the torso at a radius of 150mm, which is significantly higher than the other joints. This has been done to represent a kayak skirt, often attached to the kayak itself, and made of hydrophobic material, the kayak skirt effectively seals the inside of the kayaks hull, from the surrounding conditions, whilst being flexible enough as to not restrict the kayakers' movements.

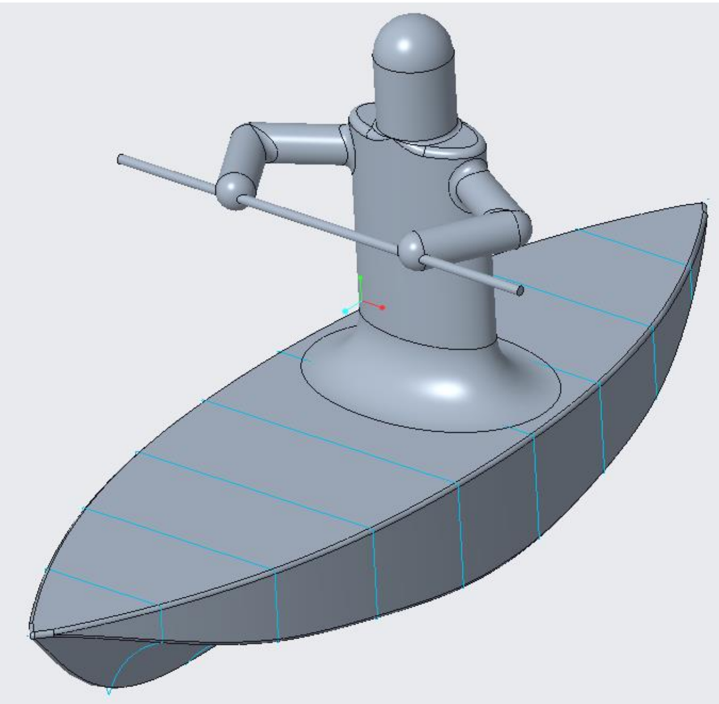

Figure 11 - Rounded Kayaker Geometry

The rounded kayak geometry can be seen in Figure 11, in addition to an added pole. The added geometry is to represent the kayakers paddle, it is a cylinder of a 25mm diameter and total length of 1.25m. The geometry is symmetrical across the kayaks centre plane, and the centre axis of the pole is coincident with the centre of the hemispherical arm ends.

3.5. Geometry, Meshing and Setup

Once the major modelling tasks, the free surface, the kayak, and the kayaker, had been completed they needed to be combined appropriately before simulations could begin. The model of the free water already exists in Ansys, however the kayaker model needed to be imported. The Creo version used in this study, 8.0.4.0, is directly supported by the ANSYS version used, 2023r1. This is ideal as the Creo .prt file with the kayaker geometry can be directly imported into ANSYS Design Modeller, in full detail, instead of converting the file to another type, such as a .step file, which can result in minor geometry changes.

The major consideration is therefore how to represent the geometry in the simulation volume. As previously discussed in the modelling stages, the only part of the kayaker geometry that is practically useful is the surface, as it interacts directly with the fluid. This meant that the rest of the geometry could be removed from the volume entirely. This can be achieved in Design Modeller, by using a body operation function, called cut material, and applying it to the imported geometry. The result is a kayaker shaped void in the geometry, that fluid must flow around. The surface between this void and the remaining volume can be defined as a surface, to which properties, such as frictional coefficients can be applied. This surface can also be used to measure, for values such as drag force or coefficient.

The mesh methodology largely remained the same after including the new geometry with two major exceptions. Firstly, the volume containing the refined mesh was increased. When considering the free surface model, the mesh was only refined at the free surface as this was the only space the fluids interacted with anything. Once the new geometry was introduced many new fluid interactions occurred, mostly effecting the flow profile at the geometries surface, however also impacting the flow upstream, downstream, and laterally around the geometry. The refined mesh size has therefore been applied to the full height and width of the geometry, starting 5m in front and behind the centre of the kayak, as shown in Figure 12. After some initial model testing the second meshing change to remove the mesh adaptation was chosen. It was observed in testing that since the additional geometry had been added the mesh adaptation had been increasing the mesh size, at greater rate. This was likely necessary due to the added complexity; however, mesh sizes were at times growing to be over 100 times larger than their initial size. Even whilst using 64 cores on the HPC, it became clear that some mesh size limitations would need to be imposed to generate results within a reasonable time frame, and the mesh adaptation was therefore disabled.

Figure 12 - Volume refined mesh regions.

All the major steps in the simulation setup remained identical, open channel flow was still used, with a 0.01s timestep and a standard initialisation with a patch for the second phase. The simulations were however no longer being used to generate a simple phase diagram, instead data needed to be generated to compare the drag properties at different flow parameters. The surface of the geometry, defined as the surface between the volume and the removed volume, was labelled as the kayak surface earlier at the geometry stage, and can now be used to calculate the total drag and the drag coefficient, experienced by the kayak and kayaker. These values can then be used to compare the effectiveness of the kayak under different ambient conditions.

3.6. Mesh and Domain Independence Studies

Once the model was developed, simulations could be run, and drag forces generated. There were however still several checks that needed to be conducted first. These were to ensure some of the previously assumed variables in both the geometry and the meshing, were suitable for this analysis, and do not negatively affect the accuracy of the model. To do this a mesh independence and domain independence study was conducted, which involved testing the model at a set simulation condition, in this case 1 m/s flow. Parameters such as element size and length were then varied and the change in results observed. If the generated results vary independently of the change, then it was determined that the value used was appropriately sized and independent of the results. Alternatively, a decision was required to compromise between both the level of accuracy and the computational time of the simulation.

The most critical study was the mesh independence study. As discussed previously the mesh adaptation study that was originally used was disabled at this point in the product. This was done as the adaptation study was increasing the mesh size far beyond the computational abilities of the available hardware. This likely meant that any mesh chosen, that will allow simulations to be solved in a reasonable amount of time, will not be completely independent of the drag force it is used to calculate. Prior to this study a 0.1m minimum element length was chosen for the finer mesh and 0.25m was chosen for the courser sized mesh areas. Given the finer meshed areas will be more critical to the simulation results, only refinement of the finer mesh was undertaken. A constant refinement ratio of 0.81 was used to generate results at five element sizes.

After conducting simulations at all five element sizes, the drag forces both increased and decreased randomly, as seen in Table 2 and were therefore not directly affected by the element size. To ensure the mesh remained independent, a maximum element size of 0.05m was chosen. As the sign of the percentage change switches at 0.0531m, this ensures that the mesh will remain independent for all future calculations.

Table 2 - Mesh Independence Study results

Min Element Size (m)	No. of elements	Drag Force (N)	Change (%)
0.1	$2.74 * 10^6$	2.0185	N.A.
0.081	$3.02 * 10^6$	2.0091	-0.4657
0.0656	$3.63 * 10^6$	1.9890	-1.000
0.0531	$4.64 * 10^6$	1.9951	0.3067
0.0430	$6.23 * 10^6$	1.9999	0.2406

The second major consideration when developing a fluid model was the upstream and downstream flow lengths. Typically, in fluid analysis, factors such as flow rate are at equilibrium across a length, given nothing externally acts upon them, however this occurs over a significantly length. In the case of this analysis the fluid flow at the inlet is represented as being perfectly split between air and water at the surface. This is not representative of the simulated free surface which forms over an appropriate distance as it approaches equilibrium. When the flow reaches the kayak, it is separated, from equilibrium, as it flows around the kayak, before gradually returning some distance behind the kayak. Should the flow not reach equilibrium either before the kayak or the outlet the flow throughout the volume will be affected.

To test this, three volume lengths were chosen in intervals of 10m. In this case the drag force reduction between the first and second testing points, 20m and 30m, was over 50%, as seen in Table 3. This was likely because the downstream length was not significant enough, at a 20m volume length, to allow the fluids to gradually rejoin after the kayak, resulting in increased lateral velocities at the rear of the kayak, increasing the total computed drag force. As this distance is increased to 30m the fluids can return to equilibrium more gradually. The percentage change at a volume length of 40m is significantly low, and therefore to save on computational time the volume length was limited to 30m.

Table 3 - Domain Length Independence Study

Volume Length (m)	Drag Force (N)	Change (%)
20	4.52	N.A.
30	2.17	-52.0
40	2.02	-6.91

When considering flow separation around an object, such as a kayak, it is important to consider not only how far up and down stream these travels, but also how far laterally around the object. To ensure the volume contained enough lateral width to model the flow accurately, another domain independence study was conducted. This involved not only changing the width of the volume but also the length of the finer mesh volume, as both are important to capturing the flow separation around the kayak. Tests were conducted at three different widths in 1m increments.

The results in Table 4 show that between different kayak widths, the measure difference in drag force is negligible, and may increase or decrease. This suggests that the volume width is completely independent of the results at a width of 5m, or possibly less. The width was maintained at 5m; to be certain the results were independent of this parameter and because changing the width did not greatly increase the computational time of the simulation.

Table 4 - Domain Width Independence Study

Volume Width (m)	Drag Force (N)	Change (%)
3	2.22	N.A.
4	2.14	-3.60
5	2.17	1.38

3.7. Testing Kayak Speeds with Headwinds.

Before testing the kayak model at a variety of conditions it was important to establish a baseline drag level. This could be achieved at a set speed; however, a kayaker's speed will often change across the length of a race. All kayakers start stationary and will often conserve energy throughout a race before pushing towards the end. The ideal speeds will change based on the length of the race, and for this research it was aimed at covering a variety of speeds across all events. To determine the highest possible k1 speed the men's 200m, the shortest race distance, was considered. (House c. 2024) The world record in the men's 200m k1 is 33.380s, by Liam Heath in 2017. His time equates to an average speed of 5.99 seconds; however, his peak speed is likely higher. Based on this it was decided that the model should cover kayak speeds up to 8m/s.

The developed CFD model does not allow the kayak to move, however this is not required to accurately calculate drag based on the kayaks speed. Only the fluid velocity, relative to the kayak, is required to calculate drag, therefore a stationary kayak can be used to generate the results for a moving kayak by increasing the magnitude of the velocity. It is important to understand that this will also affect all other objects in the volume equally. Generally, for most CFD simulations there is only one object in the volume to reduce the complexity, however the walls of the volume can also affect the solution. In the case of the kayak simulation, beyond the volume there are no walls, only more fluid. To model this effectively a similar approach can be taken as done with the kayak, where only the relative speed between the fluid inside the volume and beyond the volume, needs to be represented. Assuming that the ambient conditions are completely constant, the relative speed should be zero. As the fluid speed is already dependent on the kayak's velocity, a velocity will need to be applied to the wall to match the velocity of the fluid. In fluent instead of manually adjusting the velocity of the wall for each simulation, the wall speed can be automatically updated by defining it relative to the adjacent cell zone, which in this case was always zero.

Once the baseline measurements were taken at each kayak speed, further results needed to be developed to model how ambient conditions impact the kayak. This process was started by focusing on modelling only how magnitude effected the drag force present, a direct headwind was chosen as representative of a worst-case scenario. Since the inlet velocity in the model was coupled to the relative velocity between the flow and the kayak and the two velocities are acting in the same direction, the relevant wind velocity was simply added to the baseline velocity to produce the desired results. To determine the range of ambient conditions, present at an Olympic k1 event, Brisbane was chosen as a relevant upcoming Olympic Games location. The Australian Governments Bureau of Meteorology (2024) records climate statistics which show mean wind temperatures reaching up to 25.3 km/h, or 6.94 m/s. Like with the kayak speeds, as this is an average measure it was assumed that the peak wind speed may be far higher, at up to 10 m/s. The kayaks relative velocity may therefore reach up to 18 m/s. Testing was completed in increments of 1 m/s up to this maximum velocity.

3.8. Testing Crosswinds.

To test the effects of crosswinds on the model, instead of adding the wind velocity to the kayaks speed, the ambient flow needed to be specified at a different direction, perpendicular to the kayak. This was achieved by specifying one side of the volume as the new inlet and the opposite side as an additional surface for the outlet. When completing headwind simulations, cases such as a 2 m/s inlet speed could be used to test both, a kayak velocity of, 2m/s without wind and 1m/s with 1m/s winds. This is no longer possible for the crosswind testing, meaning to achieve the 1m/s flow increments used for the headwind simulations, over 4 times as many simulations would be required. The increments for both velocity and flow speed were therefore increased to 2m/s.

Additional consideration was required, to ensure that both the mesh and the domain remained independent of the results. Since the mesh was already determined to be independent, in the previous mesh study, it remained unchanged for the following analysis. When considering the domain there were four major considerations, length, width, height, and the dimensions of the finer meshed regions. Given an additional inlet was added to the volume, the width needed to be increased to provide the required upstream and downstream length. Given the slenderness of the kayak, it was assumed that a volume width of 30m, to match the volume length, would be sufficient for the new model. The length and width of the finer mesh volume at the centre of the domain were also matched, at 5m, creating a domain that is parallel across both major vertical planes. At the cross section of each of these planes the distribution of finer mesh regions is consistent with that of Figure 12, were the finer mesh cells are shown in the green regions.

4. Results

4.1. Overview

The following section summarizes the simulation results using the previously stated methodology. The testing was conducted in three major stages, firstly general flow rate testing, which was used to establish expected trends. This was expanded upon to test the full range of headwind data points, before finally using the adapted methodology to find cross wind results. The results are all summarised in tables and presented in matching graphs to help visualise trends. Some additional figures are provided, such as residual plots and drag monitors, to discuss potential causes of errors found in the results.

4.2. Kayak Velocity Results

The kayak velocity simulations tested a range of relative velocities up to 10m/s, in increments of 1m/s. All the simulations were able to solve, gradually reaching convergence around the 8th timestep, as shown in Figure 13. Comparing this to the drag force trends, shown in Figure 14, a large dip can be seen in the graph, at approximately 0.08s, the 8th timestep. This appears to be an oscillation, as seen with damped vibration. The solution therefore may have reached equilibrium slightly before, or after, the 8th timestep, however overshoots the result and requires some more time to settle.

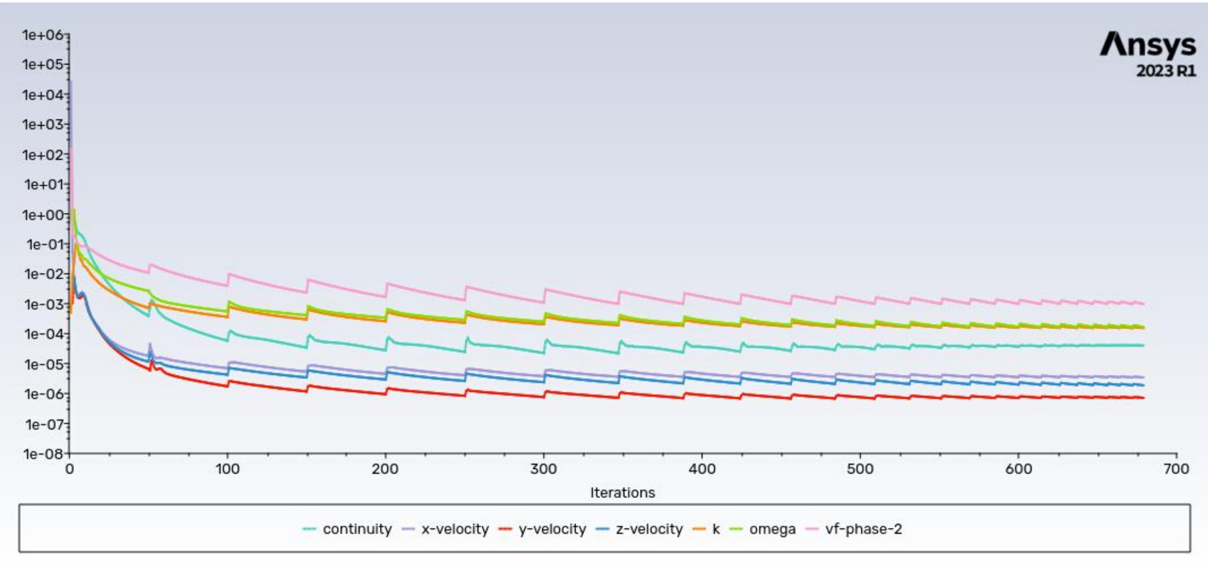

Figure 13 - 1D flow residuals.

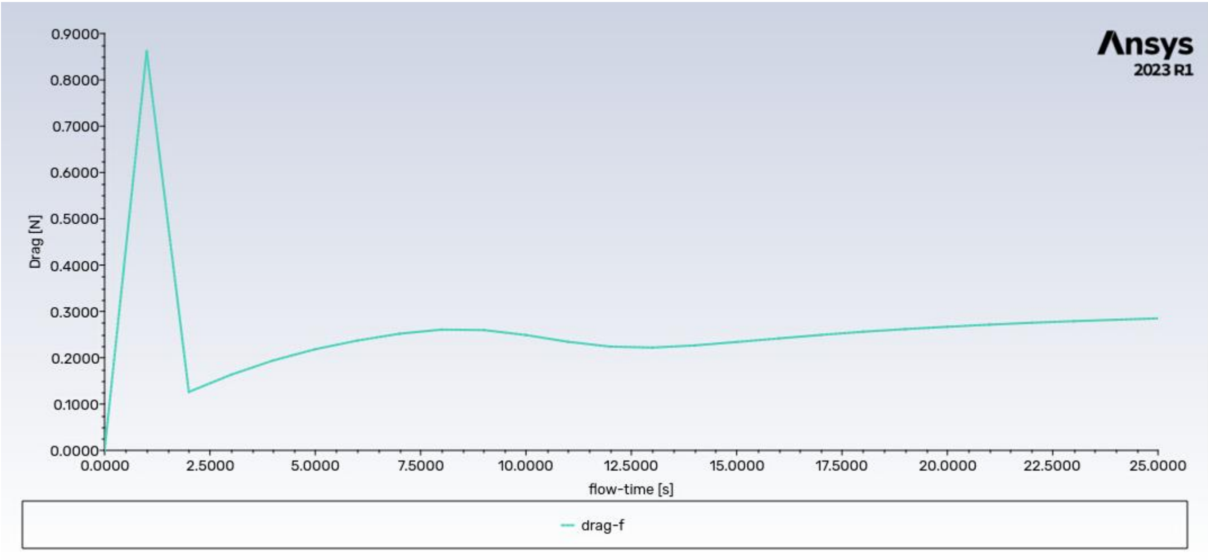

Figure 14 - Kayak Velocity Drag Monitor

The results can be seen in Table 5 below, and as expected follow a generally consistent upwards trend. Given drag is proportional to velocity squared, as shown in Equation 1, a polynomial trend should be expected. Additionally, although it was not a measured data point, assuming perfect conditions the kayak would have no drag at zero velocity. Therefore, when graphing the data, as shown in Figure 15, the trendline should intercept the origin. The resulting R^2 value of 0.9934, suggests the simulation results are highly representative of the expected polynomial trend.

Table 5 - Kayak Velocity Results

Kayak Velocity (m/s)	1	2	3	4	5	6	7	8	9	10
Drag (N)	2.1766	4.3466	7.6946	11.789	16.897	23.581	30.464	41.621	56.833	62.886

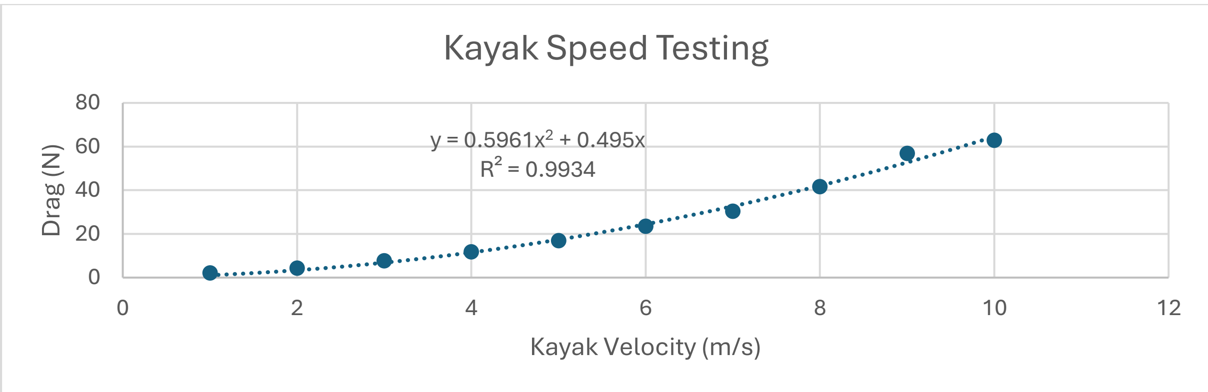

Figure 15 - Kayak Velocity Graph

The results do however appear to become less ideal at the higher kayak velocities. To better understand this, compare Figure 16 and Figure 17 which show a pressure contour graph at the centre of the simulation volume, for the 5m/s and 10m/s tests respectively. In Figure 16, it can be seen that the pressure changes gradually across the volume, whereas in Figure 17 the pressure increases suddenly, directly before the kayak, suggesting far greater disruption to the flow. To better understand why this occurs the velocity should also be considered.

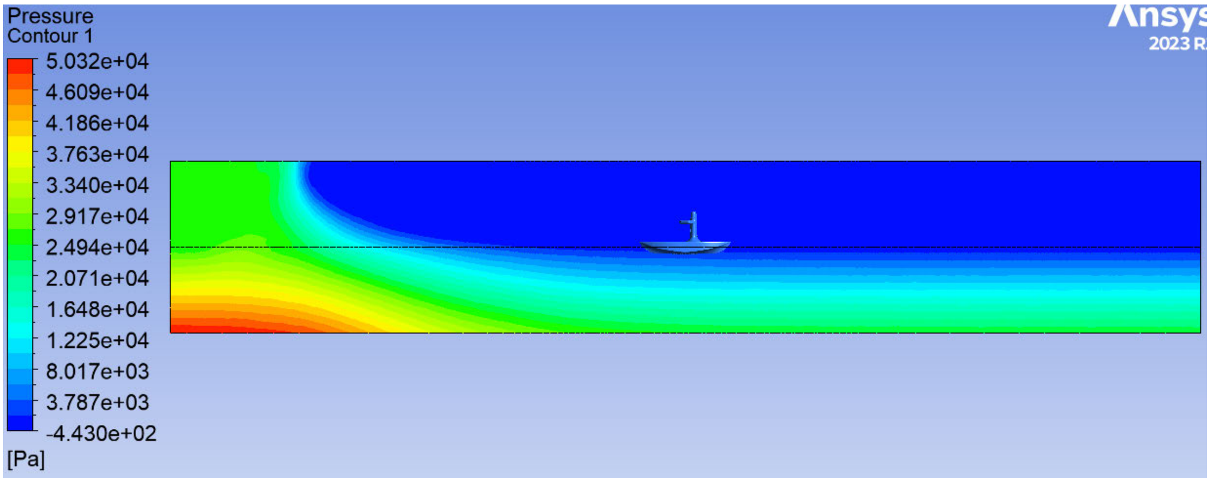

Figure 16 - 5m/s Pressure Contour

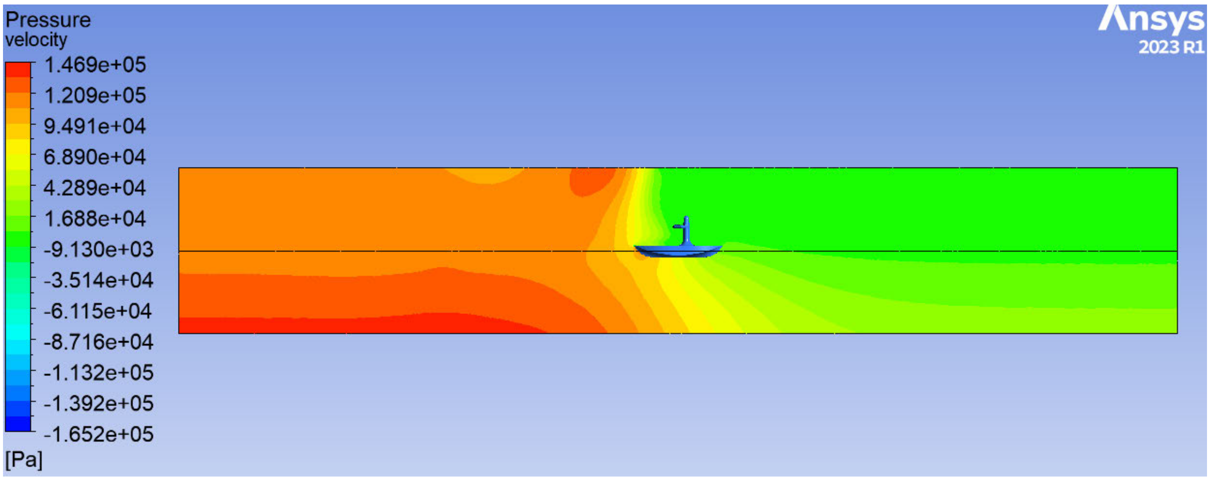

Figure 17 - 10m/s Pressure Contour

Compare Figure 18 and Figure 19, which show a velocity contour graph at the centre of the simulation volume, for the 5m/s and 10m/s tests respectively. At 5m/s the flow velocity reaches equilibrium just before being disturbed by the kayak and settles again before reaching the outlet. At 10m/s the flow is far less consistent leading up to the kayak and spikes in velocity rapidly, directly above the kayaker's head. Given the flow returns to equilibrium before reaching the outlet, there is sufficient downstream length in the volume. Additionally knowing that generally less upstream length is required, that is also unlikely to cause of an error. The problem could however be caused by insufficient volume width, which would mean that there is not enough space around the kayak to simulate the full extent of the displaced fluid.

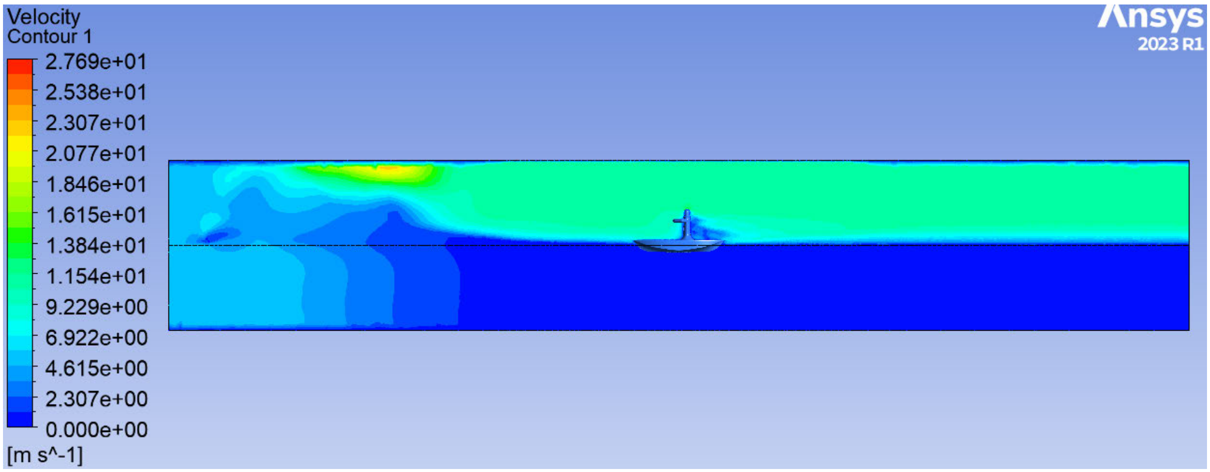

Figure 18 - 5m/s Velocity Contour

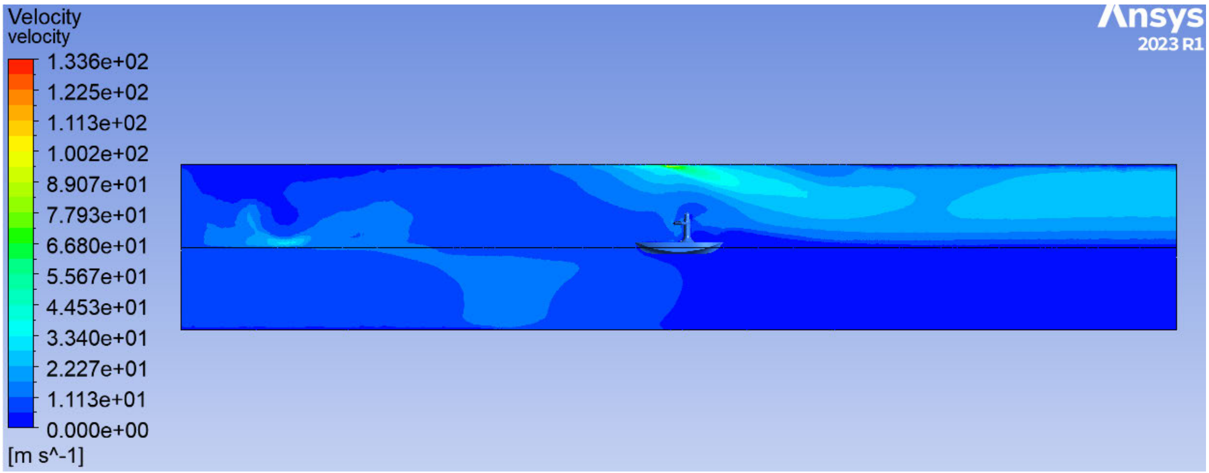

Figure 19 - 10m/s Velocity Contour

If this were to occur the simulated flow would act more restrained, as if it were inside a pipe. A disturbance in a pipe would reduce the cross-sectional area available to the flow, requiring the average velocity of the fluid to increase to maintain the same flow rate. Considering Bernoulli's equation (Princeton.edu c. 2024), since there is no elevation change, assuming constant density, a pressure increase would be required before the kayak, as seen in Figure 17, to facilitate the increased average fluid velocity at the kayak. This would force much of the flow away from the kayak toward the edges of the volume, explaining the velocity spike in Figure 19.

The domain independence study conducted during the methodology was designed to prevent such an error from occurring. This study was however conducted at a 1m/s flow rate, and therefore did not consider the full magnitude of the model's requirements. Interestingly the errors seem to only occur above the free surface of the volume, where the flow is primarily air. Since air has a low density, relative to water, it is expected that the flow above the free surface will be disturbed more easily and to a greater degree. Density is however also a factor in the magnitude of drag, meaning that the air component, and its associated errors, will have lesser effect on the results, than the water.

4.3. Kayak Headwind Results

As the methodology used for testing the kayak at different speeds without wind, is identical to that used to simulate with headwinds, many of the previous results could be reused. The remaining required tests were for eight inlet velocities from 11 m/s to 18 m/s. In Table 6, it can be seen how results from the same relative velocity are distributed across the dataset. Figure 20, breaks this data set into various subsets, to show drag variation with respect to headwind velocity, at each of the previously tested kayak velocities. It was expected that the same polynomial trend will be present on Figure 20 as was shown on Figure 15. It was also expected that the consistency of the results would continue to reduce as higher velocity magnitudes were tested.

Table 6 - Headwind Results

Drag (N)		Kayak Velocity (m/s)								
		0	1	2	3	4	5	6	7	8
Headwind Velocity (m/s)	1	2.1766	4.3466	7.6946	11.789	16.897	23.581	30.464	41.621	56.833
	2	4.3466	7.6946	11.789	16.897	23.581	30.464	41.621	56.833	62.886
	3	7.6946	11.789	16.897	23.581	30.464	41.621	56.833	62.886	80.658
	4	11.789	16.897	23.581	30.464	41.621	56.833	62.886	80.658	97.904
	5	16.897	23.581	30.464	41.621	56.833	62.886	80.658	97.904	113.4
	6	23.581	30.464	41.621	56.833	62.886	80.658	97.904	113.4	141.29
	7	30.464	41.621	56.833	62.886	80.658	97.904	113.4	141.29	136.2
	8	41.621	56.833	62.886	80.658	97.904	113.4	141.29	136.2	193.78
	9	56.833	62.886	80.658	97.904	113.4	141.29	136.2	193.78	328.63
	10	62.886	80.658	97.904	113.4	141.29	136.2	193.78	328.63	252.29

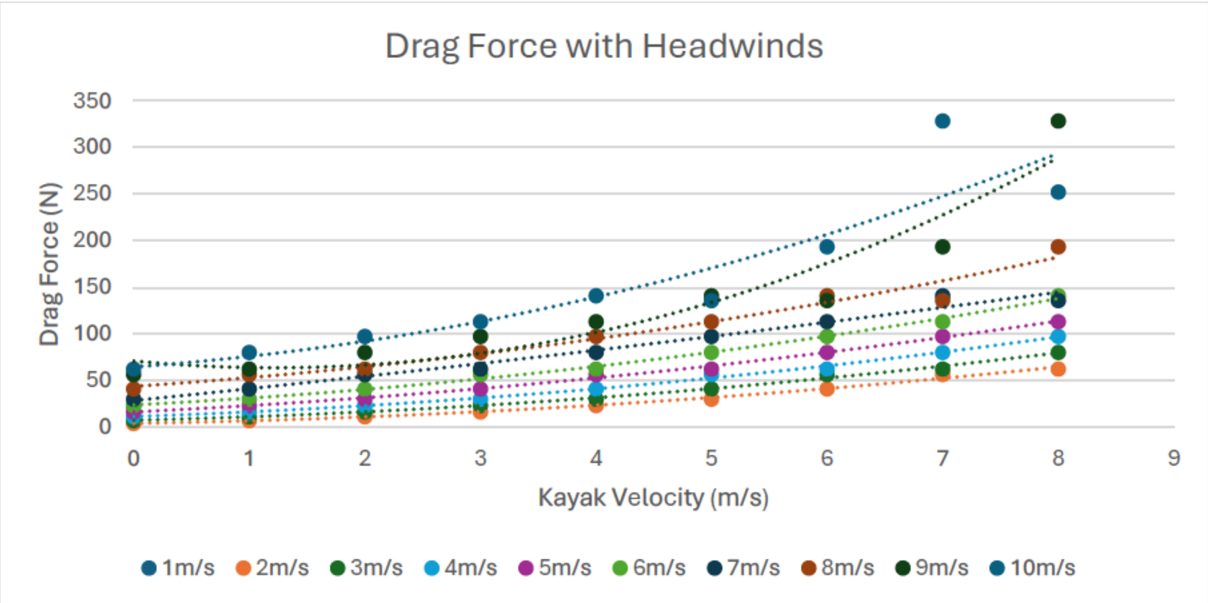

Figure 20 - Headwind Graph

Interestingly when reviewing the residuals for the test at 8m/s kayak velocity and 10m/s inlet velocity, as shown in Figure 23, the solution is reaching convergence in less iterations than that seen with lower velocities, about four iterations. The solution the system is converging to, is however not necessarily correct. Figure 21, shows the change in drag forces across each timestep, where the solution appears to reach equilibrium at the far earlier 4^{th} timestep. In Figure 14, the expected oscillation occurred at the same timestep as when the solution first converged, however Figure 21 shows the oscillation occurring far later. Solving past this point, in Figure 22, reveals the solution has begun to diverge and is certainly incorrect.

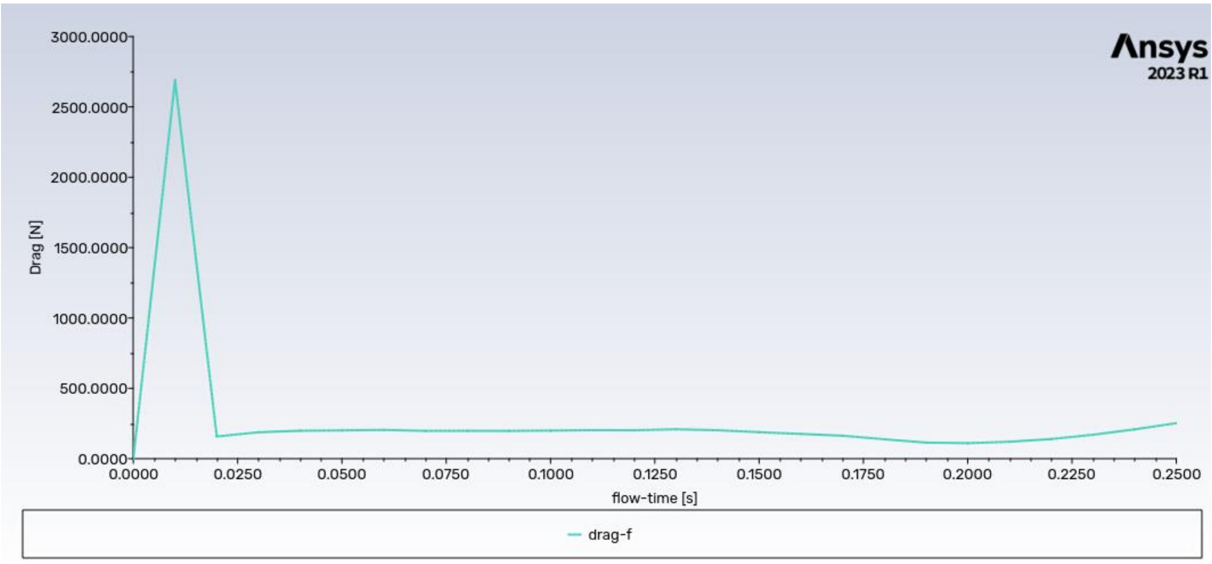

Figure 21 - High Speed Drag Monitor

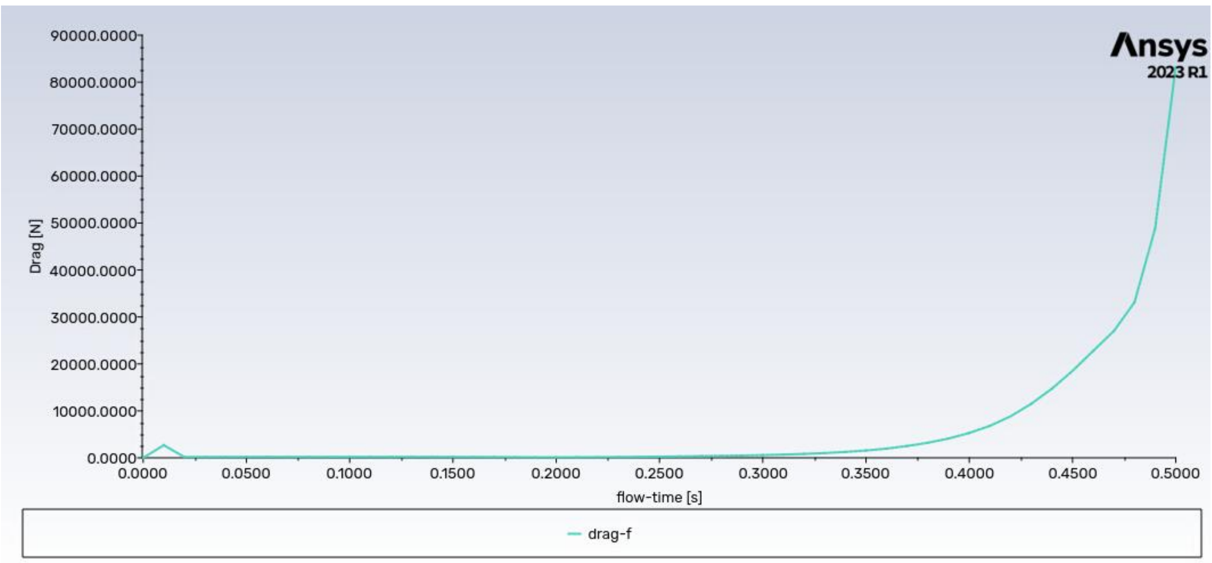

Figure 22 - High Speed Drag Monitor Extended

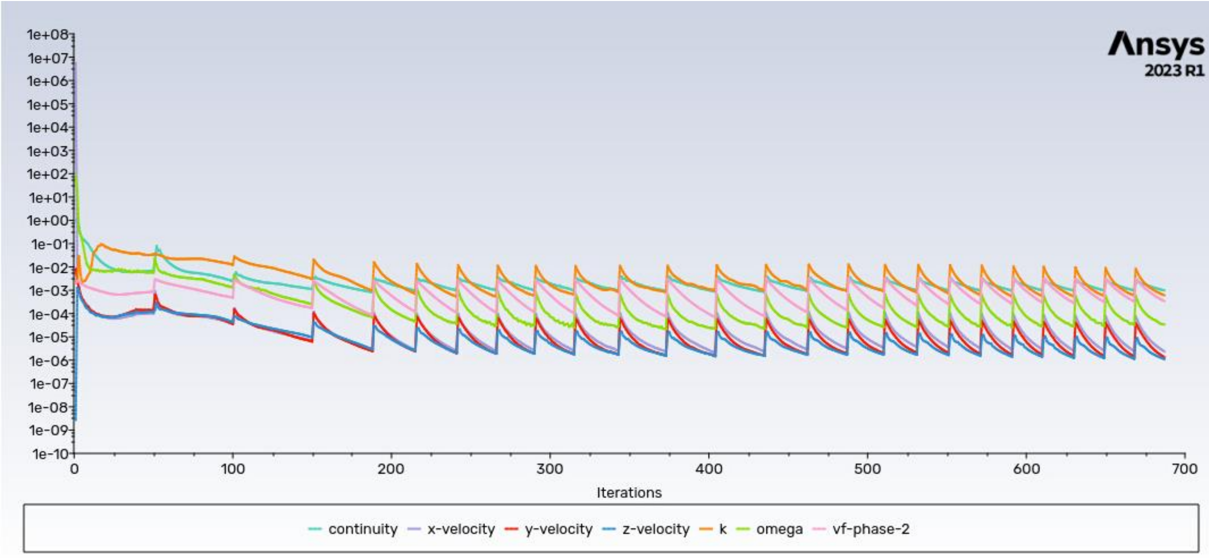

Figure 23 - High Speed Residuals

4.4. Kayak Crosswind Results

Comparative to the headwind simulations, the crosswind simulations solve far easier. As shown in Figure 24, the solution converges on the 2nd timestep, and the drag forces reach complete equilibrium only a few timesteps afterwards, as shown in Figure 25. This can most likely be contributed to the larger overall domain size used, to provide acceptable up and down stream length for the inlets and outlets.

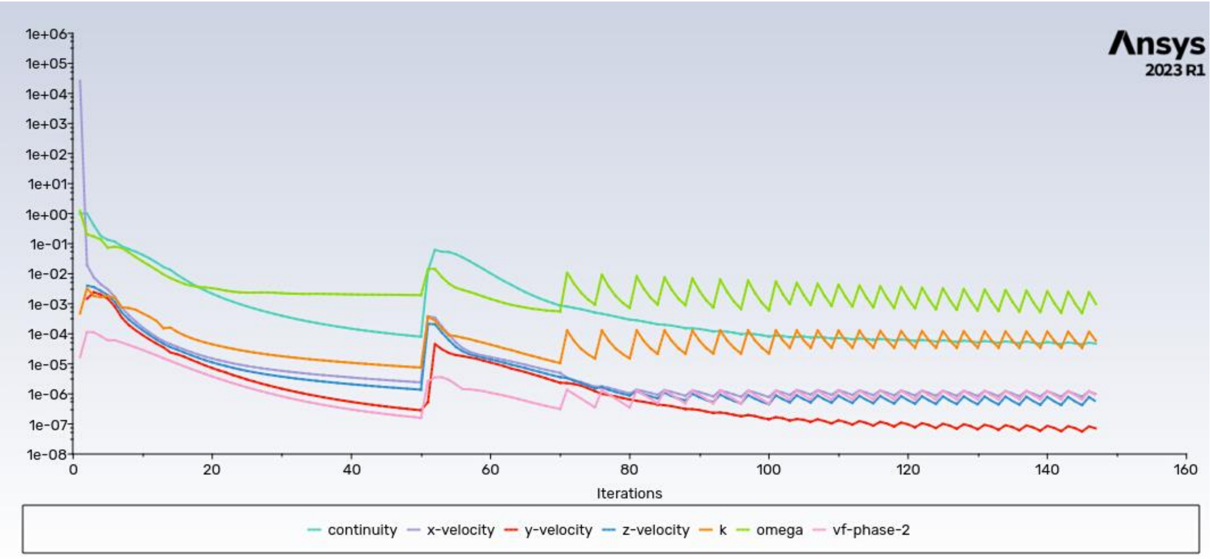

Figure 24 - Crosswind Residuals

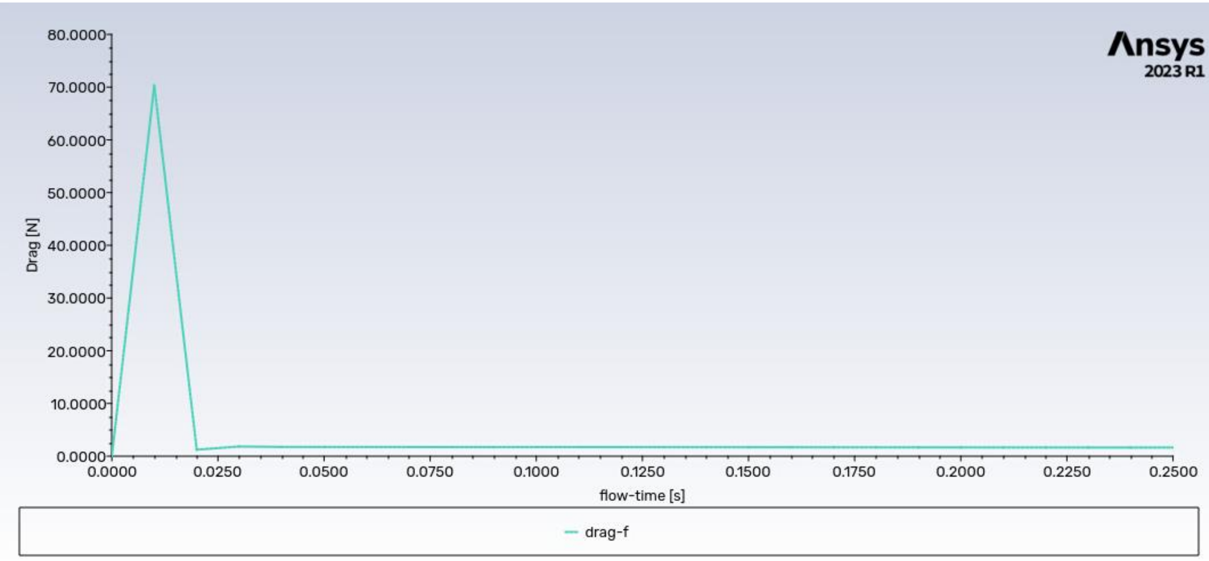

Figure 25 - Crosswind Drag Monitor

Similarly to the headwind simulations, the data has been arranged into various subsets, to show drag variation with respect to headwind velocity, at each of the previously tested kayak velocities. The results are recorded in Table 7, and are representative, not of the drag magnitude, but the total drag in the longitudinal axis of the kayak. Unlike the headwind simulations, due to the variation of inlet direction, each data point has a unique solution. The overall trend of the data is still representative of a polynomial relationship, as shown in Figure 26, however due to the change in the direction of the flow, the drag magnitude has greatly reduced. In the case of higher kayak and wind speeds, the drag forces have reduced an entire order of magnitude.

Table 7 - Crosswind Results

Drag (N)		Crosswind Velocity (m/s)				
		0	2	4	6	8
Kayak Velocity (m/s)	2	1.6486	2.0821	3.0916	4.5102	6.2345
	4	2.8473	3.7365	5.239	7.0952	9.3639
	6	4.5238	5.913	8.0108	10.313	13.135
	8	6.6531	8.7943	11.258	14.141	17.48
	10	9.2542	12.073	15.219	18.349	22.319

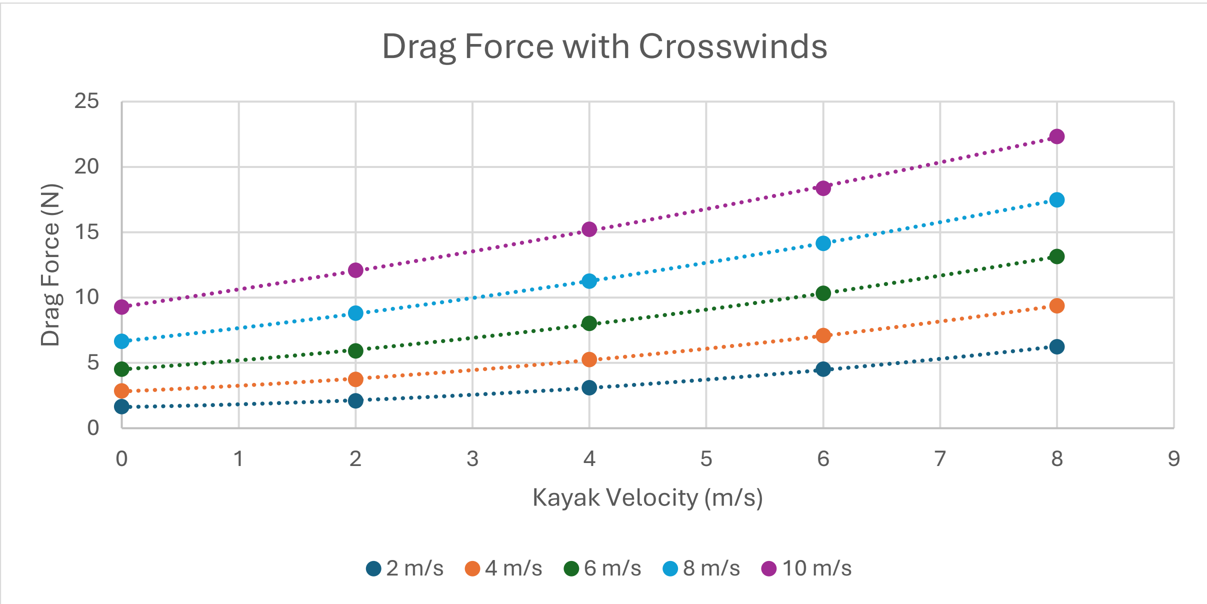

Figure 26 - Crosswind Graph

5. Discussion

5.1. Methodology

Throughout this research, the methodology was reasonably successful, due mostly to that it was developed with great consideration for the iteration from the headwind to the crosswind model. This includes consideration for the initialisation, inlets, volume boundary interactions, and free surface interactions. Where possible independence studies were used to confirm the validity of many of these assumed conditions, with some oversight to the entire scope of the simulation variance. The ultimate limitation of the methodology was the failure to consider the entire range of the potential test conditions. As the flow rate increased, other parameters in the model, in this case the volume size, were also required to increase, to fully contain the larger effected flow volume around the kayak. To avoid this in the future, best practice should be to consider the entire range of simulation conditions tested and identify a worst-case scenario. This would be a scenario, in which, at the given input, the simulation requirements for the mesh and domain are believed to be the greatest. Assuming the worst-case scenario has been accurately identified, this would mean that completing appropriate design checks, such as a mesh and domain independence study, would generate simulation requirements appropriate for the entire range of inputs.

It should also be considered that all CFD models have inherent limitations. CFD models are essentially idealised solutions of the Navier Stokes equations and different approximations are idealised for different types of flow. This means that where one model may be suitable for simulating a kayak, it likely is not suitable for simulating supersonic flow. As previously discussed, in Section 2.2.3, (Rocha Barros 2015) certain CFD solvers may initially provide accurate solutions, however not across the entire range of conditions tested in this research. This could occur for a variety of reasons, perhaps the model is not as well suited for solving turbulent flow, which occurs more easily at higher flow rates. Whilst alternate solvers could be used to obtain more accurate results, it should be noted that by using multiple solvers across the dataset the precision of the results will be greatly reduced.

5.2. Applications

Although the results show accuracy limitations at certain data points, with significantly high flow velocity magnitude relative to the kayak, this does not necessarily limit the useability of the model. Assuming the model could perfectly generate results, there would still inherently be error introduced by the user's ability to perfectly model the geometry and conditions. Excepting this limitation is essential for a user to understand how the model can be useful as a tool.

To better understand how the model can be utilized as a tool for race strategy optimisation, a scenario can be considered. Consider, a kayaker has faced a 6m/s headwind in their heat, and maintained an average velocity of 4 m/s. The athlete is to compete again, in a second heat, the following day, with a predicted 3m/s headwind. Assuming the athlete wishes to maintain their current stroke rate, considering the results in Table 6, they should expect to maintain an average speed of 7m/s in the following race. Consider that another athlete completed their heat with an average speed of 5m/s, they were however only facing a 4m/s headwind. The second athlete overcame 90.375% of the drag experienced by the first athlete in the first heat and will therefore need to increase their stroke rate to beat the first athlete in the second heat.

This sort of performance comparison is useful for tracking the performance of athletes, across the course of large events such as the Olympics. Generally, athletes race paces do not vary by multiple metres per second and therefore should the model be used for this purpose the range of the dataset generated, could be greatly reduced. This would allow data points to be generated more frequently across the velocity range, allowing for finer tracking to a higher level of precision.

To better understand how the model can be utilized as a tool for design optimisation, see Figure 27 and Figure 28. Both contours show the magnitude of the drag force acting directly against the motion of the kayak, on both the kayak and kayaker, through use of a gradient colour scale defined on the left-hand side of each figure. As seen in Figure 27, despite aerodynamic drag being relatively low compared to hydrodynamic drag, the drag forces on the kayaker's body are still significant due to its stout, non-aerodynamic shape which causes large flow separations. It is important here to notice that the drag is reduced lower on the kayaker's skirt, therefore whilst the skirt is generally used for preventing water ingress into the hull in recreational applications, it is seen here to have an aerodynamic performance benefit for the athlete. Given this a design engineer may use the model to optimise the height of the kayaker's skirt, although focus is usually on the hull.

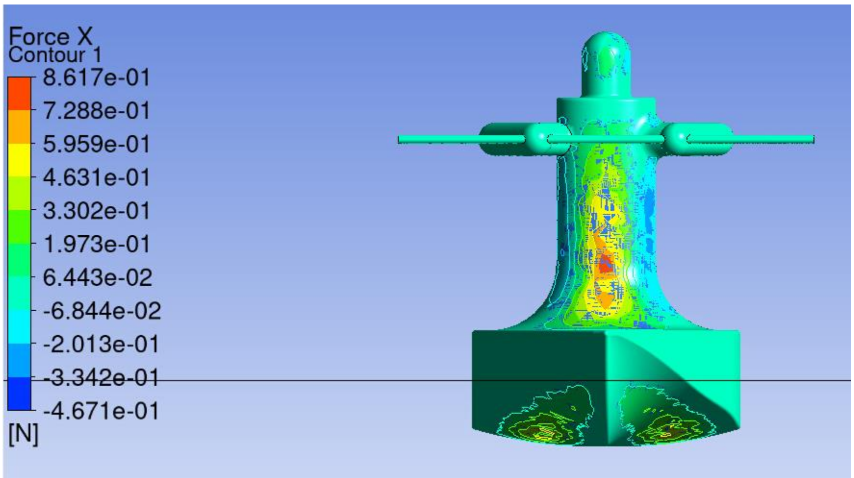

Figure 27 - Force Contour (10 m/s)

Figure 28 shows an angled underside view of the hull, which demonstrates the intentional hydrodynamic imperfections of the fishing kayak. Drag is shown to increase dramatically through the channelled sections in the hull. Using this information changes can be made to the profile of the hull to make it slenderer, before generating a new surface contour and analysing the changes. To make this process more time effective, designers may also choose to reduce model variables such as mesh size, understanding that whilst this will reduce the accuracy of their solutions, it will also reduce computational time. As the design approaches finalisation accuracy can be increased as more precise results are needed.

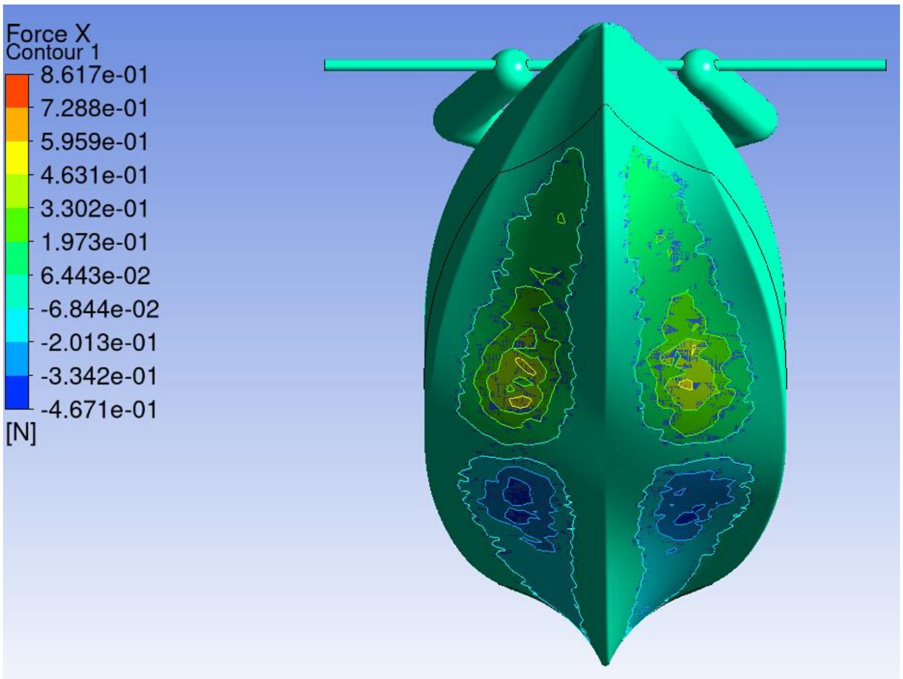

Figure 28 - Force Contour Underside (10 m/s)

6. Conclusions

This report has covered the research of using computational fluid dynamics to simulate the effects of multiphase fluid flow, around a model of a kayak and kayaker, to analyse performance at a variety of different ambient conditions. To complete this research a literature review was first conducted, to identify past findings and knowledge gaps, learn the development path of kayaks, and to understand kayak performance. This information was useful in the development of a methodology, which was considerate of key performance limitations and generated useful results that were applicable to key applications.

The methodology contained three major stages, firstly the development of an appropriate CFD model, which could accurately represent the interactions between fluids at the water surface. The additional two steps require the modelling of both the kayak and the kayaker. The kayak was able to be modelled by measuring the shape and size of a real fishing kayak, and whilst the inaccuracy of the style of kayak, when compared to typical Olympic models, would present accuracy issues for the results, a high level of precision was presented, for the specific model of kayak used. Some small assumptions were also made that both simplified the geometric shape of the kayak, whilst making it generally more representative of an Olympic k1 kayak. The modelling of the kayaker involved far more assumptions, as human geometry is fundamentally more complex. Assumptions were therefore made in this case around both size and shape by using available body measurements, and applying them to a model containing human geometry, approximated by a combination of many more simple geometric shapes. The created kayak, kayaker and fluid models were then combined and used to simulate the results. The final domain had to vary slightly, to create a model that was appropriate for testing flow at various directions. Multiple mesh and domain independence studies were conducted, to confirm the assumed values had no influence over the results.

Following the methodology, results were generated with minimal issues. Collecting and graphing all the data points together, revealed trends in the generated data set, which correlated with what was expected by the relevant theory. In exception to this were some of the trendlines in the headwind testing. Given that the velocity of the ambient flow and kayak motion were acting in the same direction, this resulted in the highest velocity magnitude, relative to the kayak. This high magnitude is believed to have exceeded the capabilities of the solver used, resulting in some inaccuracies in the results. Despite this it was shown that the generated results were still incredibly useful, as a tool for analysing the race pace of competitors across multi-race events, which occur at a variety of times and conditions. This can be used to inform decisions regarding race strategy.

Reflecting on the project it has been generally successful at meeting the original project aim, to create a Computational Fluid Dynamics (CFD) model to analyse the effects of dynamic ambient conditions, present during a competitive flatwater kayak sprint, on the overall performance of the kayaker. After completing the project there are, however, a variety of changes that could be made to the methodology, to improve the accuracy of the results and expand the scope of the project for future research. The addition of stroke modelling would be a major area of improvement, (Morgoch, Galipeau & Tullis 2016) given that the stroke forces are significant enough to overcome the drag on the kayak, they inevitably have a significant effect on the flow around the kayak. (Banks et al. 2014) Techniques for achieving this have already been documented by other researchers, and could be added to the existing model, without considerable changes.

Significant improvements could also be made to the physical modelling of both the kayak and kayaker. To more effectively model the kayak, a representative Olympic k1 kayak should be used. It should be achievable to gain access to such a kayak for modelling now that the potential research applications have been demonstrated. Additionally, the use of a more suitable 3D CAD measuring device, such as a LIDAR scanner, would allow for more accurate and frequent measurements to be taken of the kayak, without significantly increasing the time invested. This would also eliminate the need for geometric simplifications to be made. Applying a similar methodology to modelling the kayaker would require again using a 3D scanner, instead to model the physical geometry of an Olympic level kayaker, or other athlete of a representative physical build.

The previously stated improvements would all be suitable for improving the accuracy of the results however, as demonstrated in the discussion, given a suitable level of precision is achieved, the results can still be useful as tool. As discussed, the effectiveness of the tool is fundamentally limited by how it is used by the operator, and with this in mind improvements can be made to allow the model to be better applied. In this case a major improvement would involve uncoupling the inlet properties for both the air and the water, allowing operators to specify different magnitudes and directions for the velocity of each fluid. The model in theory already contains this capability however this was not completed under the limited scope of this research. Additional validation would be required to ensure the suitability of the model for generating such results.

7. Bibliography

Bagué, A, Degroote, J, Demeester, T & Lataire, E 2021, 'Dynamic Stability Analysis of a Hydrofoiling Sailing Boat using CFD', *Journal of Sailing Technology*, vol. 6, no. 01, pp. 58-72.

Banks, J, Phillips, AB, Turnock, SR, Hudson, DA & Taunton, DJ 2014, 'Kayak blade–hull interactions: A body force approach for self-propelled simulations', *Proceedings of the Institution of Mechanical Engineers, Part P: Journal of Sports Engineering and Technology*, vol. 228, no. 1, pp. 49-60.

Barber, HL 2018, 'Effects of Wind in the Field of Play for Elite Sprint Kayakers', Cerleton University, Carleton Universtiy Institutional Repository.

Barreto, L 2020, *How F1's new sliding scale aero testing rules work – and what impact they will have on racing*, Formula1.com, viewed 08/06, <https://www.formula1.com/en/latest/article/how-f1s-new-sliding-scale-aero-testing-rules-work-and-what-impact-they-will.pn0sG8N4A0cjbNRbdYx8a>.

Benson, T c. 2024, *The Drag Equation*, grc.nasa.com, viewed 25/07, <https://www.grc.nasa.gov/www/k-12/VirtualAero/BottleRocket/airplane/drageq.html>.

blazinpaddles 2017, *A BRIEF HISTORY OF KAYAKING*, [2024], viewed 02, <https://www.blazinpaddles.com/a-brief-history-of-kayaking/#:~:text=The%20first%20kayaks%20were%20rudimentary,animal%20skins%2C%20bones%20and%20wood>.

Canoe Flatwater, 2023, International Olympic Commitee, Olympics.com, viewed 05/10, <https://olympics.com/en/sports/canoe-kayak-flatwater/>.

Caplier, C, Gomit, G, Rousseaux, G, Calluaud, D, Chatellier, L & David, L 2019, 'Calibrating and measuring wakes and drag forces of inland vessels in confined water in a towing tank', *Ocean Engineering*, vol. 186, p. 106134.

Castillo, HA 2022, 'Best Uses For A Kayak', *sharkwatersports.org*, 21/11/2022, <https://sharkwatersports.org/2022/11/21/best-uses-for-a-kayak/#:~:text=You%20can%20use%20it%20on,by%20people%20of%20all%20ages.>.

Day, B c. 2024, 'What Are The Different Types Of Kayaks', <https://paddlingmag.com/skills/buying-advice/types-of-kayaks/#Types_of_kayaks_by_design>.

Georgios D. Tzabirus, Stylianos P. Polyzos, Konstantina Sfakianaki, Vasilios Diafas, Athanasios D. Villotis, Konstantinos Chrisikopoulos & Kaloupsis, S 2010, 'Experimental and Numerical Study of the Flow Past the Olympic Class K-1 Flat Water Racing Kayak at Steady Speed', Universidade da Beira Interior (Portugal).

Gomes, BB, Machado, L, Ramos, NV, Conceição, FA, Sanders, RH, Vaz, MA, Vilas-Boas, JP & Pendergast, DR 2018, 'Effect of wetted surface area on friction, pressure, wave and total drag of a kayak', *Sports biomechanics*, vol. 17, no. 4, pp. 453-61.

Hanna, RK 2012, 'CFD in Sport-a Retrospective; 1992-2012', *Procedia engineering*, vol. 34, pp. 622-7.

Harrison, SM, Cleary, PW & Cohen, RC 2019, 'Dynamic simulation of flat water kayaking using a coupled biomechanical-smoothed particle hydrodynamics model', *Human movement science*, vol. 64, pp. 252-73.

House, TC c. 2024, *World Records in Canoe Sprint*, viewed 10/08, <https://thecanoeinghouse.com/canoeing-world-records/>.

Instruments, N c. 2024, *Surface and Interfacial Tension*, nanoscience.com, viewed 25/07, <https://www.nanoscience.com/techniques/tensiometry/surface-and-interfacial-tension/#:~:text=The%20increase%20in%20temperature%20causes,C%20is%2072.0%20mN%2Fm.>.

Intel 2023, *Moore's Law*, Article, viewed 08/06, <https://www.intel.com/content/www/us/en/newsroom/resources/moores-law.html#gs.aj21aw>.

Iqbal, M, Terziev, M, Tezdogan, T & Incecik, A 2024, 'Unsteady RANS CFD Simulation on the Parametric Roll of Small Fishing Boat under Different Loading Conditions', *Journal of Marine Science and Application*, vol. 23, no. 2, pp. 327-51.

Jonathan R. Potts & William J. Crowther 2000, 'Disc-wing Aerodynamics', The University of Manchester, UK.

Leroyer, A, Duvigeau, R, Queutey, P, Crochet, J-P & Rouffet, C 2016, 'Toward optimization using unsteady CFD simulation around kayak hull', *Procedia engineering*, vol. 147, pp. 293-8.

Leroyer, A, Robert, Y, Duvigneau, R, Queutey, P & Visonneau, M 2016, 'The use of High-Performance Computing in nautical sports with a focus in hydrodynamics on rowing and kayaking', *Sports Physics*.

Lukes, RA, Hart, JH, Potts, J & Haake, SJ 2014, 'A CFD Analysis of Flow Around a Disc', *Procedia engineering*, vol. 72, pp. 685-90.

Mantha, VR, Silva, AJ, Marinho, DA & Rouboa, AI 2013, 'Numerical Simulation of Two-Phase Flow Around Flatwater Competition Kayak Design-Evolution Models', *Journal of Applied Biomechanics*, vol. 29, no. 3, pp. 270-8.

McDonnell, LK, Hume, PA & Nolte, V 2013, 'A deterministic model based on evidence for the associations between kinematic variables and sprint kayak performance', *Sports Biomech*, vol. 12, no. 3, pp. 205-20.

Meteorology, Bo 2024, *Summary statistics BRISBANE AERO*, <http://www.bom.gov.au/climate/averages/tables/cw_040842.shtml>.

Mohammad, A & Majid, M 2015, 'A Review on the Drag Reduction Methods of the Ship Hulls for Improving the Hydrodynamic Performance', *International journal of maritime technology*, vol. 4, no. Summer and Autumn 2015, pp. 51-64.

Morgoch, D, Galipeau, C & Tullis, S 2016, 'Sprint canoe blade hydrodynamics-modeling and on-water measurement', *Procedia engineering*, vol. 147, pp. 299-304.
Outfitters, F c. 2024, *Kayak Materials and Their Evolution*, frontenacoutfitters.com, viewed 14/05, <https://www.frontenacoutfitters.com/blogs/tutorials/kayak-materials-and-their-evolution>.
Pladdles, B 2017, 'A Brief history of Kayaking', 20/05/2017, <https://www.blazinpaddles.com/a-brief-history-of-kayaking/>.
Pouya Jalilian, Patrick K. Kruen, MohammadHady M. Nakhmalbaf & Liou, WW 2014, 'Computational aerodynamics of baseball, soccer ball and volleyball ', *American Journal of Sports Science*.
Princeton.edu c. 2024, *Bernoulli's Equation*, viewed 02/11/2024, <https://www.princeton.edu/~asmits/Bicycle_web/Bernoulli.html>.
Robinson, MG, Holt, LE & Pelham, TW 2002, 'The technology of sprint racing canoe and kayak hull and paddle designs', *International Sports Journal*, vol. 6, no. 2, pp. 68-85.
Rocha Barros, FL 2015, 'Study of Kayak Design on Calm Water Resistance', Universidade do Porto, ProQuest.
Shen, H, Xiao, Q, Zhou, J, Su, Y & Bi, X 2022, 'Design of hydrofoil for the resistance improvement of planing boat based on CFD technology', *Ocean Engineering*, vol. 255, p. 111413.
Wang, X, Olsen, SM, Andres Martinez, E, Olsen, KN & Kiil, S 2018, 'Drag resistance of ship hulls: effects of surface roughness of newly applied fouling control coatings, coating water absorption, and welding seams', *Journal of Coatings Technology and Research*, vol. 15, no. 4, pp. 657-69.
Wüthrich, D, Shi, R & Chanson, H 2021, 'Strong free-surface turbulence in breaking bores: a physical study on the free-surface dynamics and air–water interfacial features', *Journal of fluid mechanics*, vol. 924.

8. Appendix

Appendix A. Project Specification

Title: CFD analysis of Olympic Flat-Water Sprint Kayaking at Variable Conditions

Name: Ethan Wyatt

Major: Mechanical Engineering

Supervisor: Khalid Saleh

Sponsorship: Nil

Enrolment: ENP 4111 – YL1 2024

Introduction and Background

Throughout human history aquatic travel has played a significant role in the expansion of our species. The earliest recorded civilisations all found success by settling near major rivers, as this gave them access to fresh water, and inevitably resulted in the creation of the canoe, the basis of the modern kayak. As civilisation evolved over time, we found the need to develop larger watercraft, capable of moving cargo. This development has continued to create the large cargo, passenger, and battleship technology we possess currently, however single person watercraft have not changed much at all since there creation, except for material changes.

Kayaks are believed to have first been built approximately 5000 years ago, by tribes in north America. These tribes constructed kayaks out of a variety of materials, such as either bones or wood for the frame, which would have animal skins covering it to make a waterproof hull. Earlier kayaks also generally came in a much greater variance of sizes ranging from shorter hunting kayaks, up to 60-foot kayaks that could carry families, and often used seal bladders for extra buoyancy. (blazinpaddles 2017)

The major development of kayaks has come from competitions, like the Olympic games. At the Berlin Olympic games in 1936, (blazinpaddles 2017) kayak racing was introduced for the first time. At the Olympic games athletes compete in flatwater sprints between 200m and 1000m. (*Canoe Flatwater* 2023) In this style of competition, athletes can be separated by margins far smaller than a second, therefore unlike in the manufacturing of larger vessels, kayaks designed for sports require an extremely high level of accuracy. This is however difficult as a variety of small variables at play, make design extremely challenging, when approaching the limit of performance.

Through the history of the Olympic games between 1972 and 2000 there were 3 major kayak design changes, first the Delta shaped kayak in 1972, then the eagle design in 1988, followed by the modified eagle design in 1996. (Robinson, Holt & Pelham 2002) The introduction of each of these designs, correlates to a major reduction in race times across the 1000 m. This shows just how much kayak design has improved and how great of an effect it has on the level of competition in the sport.

Ambient conditions also have a major impact on race times, and may be affected by the waters current, the wind speed and direction and its effects on the surface of the water. The conditions will determine the hydrodynamic forces acting on the hull and the resulting drag experienced by the kayak. Combining this with biomechanical information relating to the athlete, would allow the CFD model, to be a useful tool in optimising competitive race performance. (Mantha et al. 2013)

Aims and Objectives

The research being proposed will be to create a Computational Fluid Dynamics (CFD) model, to analyse the effects of dynamic ambient conditions, present during a competitive flatwater kayak sprint, on the overall performance of the kayak. By using the CFD model at an array of conditions, more general analytical models can be generated to determine the relationship between key conditional parameters, such as flow speed, and key performance parameters, such as drag, across the range of expected conditions. This information could be applied to a variety of other applications, race strategies and kayak designs, with some additional information or results.

Race strategy optimisation can be achieved, by combining the results of a CFD model, with biomechanical knowledge of the human body. In the case of kayaker performance, several conditions will affect the success of an athlete during an event, including wind, temperature, water current, elevation, and fatigue. Combining all these external factors into a CFD model, would allow coaches to make informed decisions on strategy, such as recommendations on stroke rate and length, to vary performance across different race lengths. Additionally, assessing the performance of other athletes, could improve energy conservation strategies, for later races throughout an event. By adapting this model to other vessels, such as cargo ships, the model might serve additional use to optimize fuel efficiency in powered watercraft.

Design optimisation can be achieved by generating drag contour maps on the surface of the kayaks hull. Although the kayak has existed a long time, design is mainly iterative, essentially trial and error. Physical testing has limitations, such as consistency during testing, cost of prototype production and generic performance results for the design. By using a drag contour map, designers can get a more localised understanding of exactly where their designs are limited. Assuming an appropriate knowledge of average velocities in kayaking events, design could even be optimised for different length kayaking events. This sort of precision is necessary, as modern design approaches its limits.

Expected Outcomes

- Create a CFD model capable of calculating performance metrics for a generalised kayak geometry.
- Compare the distribution of the results with respect to kayak velocity, across a variety of flow magnitudes and directions.
- Consider the potential applications of the research.
- Maintain a model that can be easily expanded upon for future research.

Resources Required

- Equipment
    - Access to the UniSQ HPC (Fawkes)
    - Personal Workstation

- Software:
    - ANSYS 2023 R1
    - Creo Parametric 8.0.4.0.
    - Endnote

- Access
    - UniSQ Library Database

Appendix B. Project Timeline

Table 8 - Project Timeline

Time	Task	Description
Month 1	Project Proposal and Planning	• Create a plan for the project, outline aims, objectives and a schedule. • Seek approval from supervisor, of project plan and all necessary resources.
Month 2-3	Literature Review	• Review past studies to determine current approaches to similar problems and their limitations. • Create a suitable methodology, based on these findings.
Month 4-5	Modelling and Meshing	• Use Creo Simulate to physically model a kayaker and their equipment. • Use Ansys Fluent to create a fluid model of an Olympic flat-water kayaking race. • Use ANSYS to import, combine and mesh all models. • Use ANSYS Fluent student licence to test and validate models at limited mesh size on personal workstation.
Month 6-7	Simulation and Analysis	• Use ANSYS Fluent on the UniSQ HPC to test and simulate models at an increased mesh size. • Analyse and compare simulation results. • Use the simulation results to develop an analytical model of kayaker race times based on strategy. • Use the simulation results to identify limitations in kayak design and suggest improvements.
Month 8	Drafting	• Organise and structure key project outcomes. • Collect all references, figures, and tables, used, or developed throughout the project. • Record report progress and results in an appropriately structured report, using professional language and formatting.
Month 9	Peer Presentation	• Summarise draft dissertation into an A1 poster, to be presented at the showcase event. • Pre-empt potential questions and prepare answers. • Attend resident school, to present project, answer questions and provide feedback to peers. • Identify current gaps and limitations of the project.
Month 10	Writing and finalisation	• Perform additional analysis and validation of the model's other potential uses, if possible, in remaining timeframe. • Incorporate any new analysis, limitations or changes identified since the draft. • Finalise the report, ensuring all required aspects are covered and the report meets a professional standard.